

**A KINETIC STUDY OF SULFATE  
REDUCTION WITH CARBON**

**Project 3473-1**

**Report One  
A Progress Report  
to**

**MEMBERS OF THE INSTITUTE OF PAPER CHEMISTRY**

**June 23, 1981**

THE INSTITUTE OF PAPER CHEMISTRY

Appleton, Wisconsin

A KINETIC STUDY OF SULFATE  
REDUCTION WITH CARBON

Project 3473-1

Report One

A Progress Report

to

MEMBERS OF THE INSTITUTE OF PAPER CHEMISTRY

June 23, 1981

# TABLE OF CONTENTS

	Page
LIST OF TABLES	iv
LIST OF FIGURES	v
SUMMARY	1
INTRODUCTION	4
Processes in a Kraft Recovery Furnace	4
Project Objectives	6
SULFATE REDUCTION CHEMISTRY	9
Basic Chemistry	9
Previous Work	11
EXPERIMENTAL SYSTEM	14
EXPERIMENTAL RESULTS	19
Carbon Surface Area Effect	20
Sulfate Effect	24
Sulfide Effect	24
Iron Catalyst Effect	26
Temperature and Melt Composition Effects	29
Carbon Rod Temperature Effect	32
Sulfate Reduction with Carbon Monoxide	36
Oxidation of Sulfide	37
Thiosulfate Reduction	38
Carbon Dioxide Reduction with Carbon	41
MECHANISM OF SULFATE REDUCTION WITH CARBON	42
Summary of Sulfate Reduction	42
Proposed Mechanism for Sulfate Reduction with Carbon	44
Reaction of Carbon Dioxide with Carbon	45
Sulfate Reduction with Carbon Monoxide	46
Decomposition of Sulfite	47

	Page
Desorption of Carbon Monoxide and Carbon Dioxide from the Melt	47
Sulfate Reduction Model	48
Effect of Carbon Dioxide on Sulfate Reduction with Carbon	53
APPLICATION TO RECOVERY FURNACE	61
Critical Kinetic Parameters	61
Activation Energy	62
Heat of Reaction	63
Heat Transfer Effects	63
Char Bed Data	67
ADL Model	73
Char Combustion	74
Overall Reduction Efficiency	76
CONCLUSIONS	78
FUTURE WORK	80
ACKNOWLEDGMENTS	81
LITERATURE CITED	82

LIST OF TABLES

<u>Table</u>		<u>Page</u>
I	Equilibrium CO <sub>2</sub> /CO Ratios	10
II	Reduction of Sodium Sulfate	10
III	Effect of Temperature on Sulfate Reduction with Carbon	29
IV	Sodium Sulfate Reduction with Carbon Monoxide	37
V	Parameters Describing Sulfate Reduction with Carbon	52
VI	Summary of Sample Analyses from Mill Visits (Weight Percent)	72

LIST OF FIGURES

<u>Figure</u>		<u>Page</u>
1	Experimental System	15
2	Experimental Reactor	17
3	Sulfate Reduction with Carbon	21
4	Effect of Carbon Surface Area on Sulfate Reduction with Carbon	23
5	Effect of Sulfate on Sulfate Reduction with Carbon	25
6	Effect of Sulfide on Sulfate Reduction with Carbon	27
7	Effect of Iron on Sulfate Reduction with Carbon	28
8	Effect of Temperature on Sulfate Reduction with Carbon	31
9	Effect of Temperature on Sulfate Reduction in $\text{Na}_2\text{CO}_3$	33
10	Effect of Temperature on Sulfate Reduction in $\text{Na}_2\text{CO}_3\text{-K}_2\text{CO}_3\text{-Li}_2\text{CO}_3$	34
11	Partial Pressure of $\text{CO}_2$ over $\text{Li}_2\text{CO}_3$	35
12	Oxidation of Sodium Sulfide	39
13	Sulfate Reduction with Carbon: $\text{CO}_2$ and CO Evaluation <u>vs.</u> Time	54
14	Sulfate Reduction with Carbon: $\text{CO}_2$ and CO Evaluation <u>vs.</u> Time	55
15	Sulfate Reduction with Carbon: $\text{CO}_2$ and CO Evaluation <u>vs.</u> Time	56
16	Effect of Carbon Dioxide Addition to Purge Stream	58
17	Effect of Carbon Dioxide on Sulfate Reduction Rate	60
18	Measured Bed Temperature - Weyerhaeuser Furnace	71

THE INSTITUTE OF PAPER CHEMISTRY

Appleton, Wisconsin

A KINETIC STUDY OF SULFATE  
REDUCTION WITH CARBON

SUMMARY

One of the key chemical reactions occurring within a kraft recovery furnace is the reduction of sodium sulfate to sodium sulfide in the hearth zone. Although this reaction is obviously important to kraft chemical recovery, relatively little information is available on fundamental characteristics of the reaction. This has led to confusion regarding conditions necessary for achieving adequate reduction in the furnace and has inhibited performance optimization.

This report presents the results of a study of the kinetics of sulfate reduction in molten carbonate salts using carbon as the reducing agent. Among the variables studied were temperature, sulfate and sulfide concentration, carbon surface area, and melt composition. The experimental results and a proposed reaction mechanism explaining those results are presented.

Reduction reactions were carried out in a batch mode using an alumina crucible containing about 1.5 liters of smelt. The crucible was contained within an iron retort in a cylindrical electric furnace. Nitrogen gas was bubbled through the molten smelt to keep the mass stirred and to sweep off product gases. Reduction was initiated by adding carbon rods about one inch in length to the reactor. The reduction rate was measured by quantitative analysis of  $\text{CO}_2$  and  $\text{CO}$  concentrations in the off-gases using an infrared spectrophotometer.

Sulfate reduction was found to be autocatalytic in that the rate of reaction increased with time. By adding initial amounts of sulfide to the reactor, it was determined that this autocatalytic behavior was not due to the increase in

sulfide during reaction. By varying the amount of sulfate added to the reactor, it was determined that sulfate reduction with carbon is first order in sulfate at low sulfate concentrations but zero order at high sulfate concentrations. By varying the amount of carbon added, the rate of reaction was found to be proportional to the square root of the carbon surface area. The activation energy for sodium sulfate reduction in a sodium carbonate melt was determined to be approximately 53 kcal/g mole. Reaction kinetics were not appreciably influenced by the nature of the carbonate cation, and hence by the melting point of the smelt or smelt fluidity.

The following mechanism is proposed to explain the experimental results. Reduction is initiated by the absorption of carbon dioxide on the surface of the carbon. The absorbed carbon dioxide then reacts with the carbon to form two molecules of carbon monoxide. These carbon monoxide molecules then desorb from the carbon and react with sulfate in the melt to produce additional carbon dioxide. The autocatalytic nature of this reaction is then due to the increase in carbon monoxide and carbon dioxide in the melt.

In parallel experiments, it was found that sulfide reoxidation is inherently faster than reduction and is controlled by oxygen mass transfer.

The results of the study have some interesting implications for recovery furnace operation. The combination of an endothermic reaction and temperature sensitive kinetics (high activation energy) means that reduction within the char bed is heat transfer limited. The single most important variable influencing reduction in the furnace is bed temperature. Reduction rates become quite low at temperatures of 1500°F (815°C), and termination of reduction reaction rather than smelt melting temperature tends to control the temperature at which smelt discharges from the furnace. The net reduction efficiency in smelt leaving the furnace depends on the



amount of reoxidation which occurs ahead of the spout as well as the degree of reduction reached in the char bed. Finally, the actual mechanism by which carbon is burned in the char bed is by reduction of sulfate, with the sulfate then being reformed by reaction between sulfide and combustion air. Air does not contact the carbon directly. This explains the difficulty in burning char in sulfur-free alkaline pulping operations.

## INTRODUCTION

One of the key reactions in kraft chemical recovery is the reduction of sodium sulfate to sodium sulfide. Although this reaction is industrially important, little information is available concerning its mechanism or controlling parameters. In a kraft recovery furnace, reduction occurs in a melt consisting principally of sodium carbonate, sodium sulfate, sodium sulfide, and carbon at temperatures in excess of 1400°F. Here molten sulfate reacts with carbon to form sulfide, carbon monoxide, and carbon dioxide. The lack of information on this reaction is due to the difficulty of studying a reaction involving three phases (solids, liquid, and gas), the high temperature required, and the corrosive nature of the reaction system.

## PROCESSES IN A KRAFT RECOVERY FURNACE

The firing of black liquor in a recovery boiler is somewhat more complex than the firing of a fossil fuel. Overall objectives are different, since recovery of the inorganic salts in a form suitable for regeneration of pulping chemicals is required as well as combustion of the organic matter for steam generation. The conversion of the inorganic material to the desired  $\text{Na}_2\text{CO}_3$  and  $\text{Na}_2\text{S}$  takes place in the char bed and occurs simultaneously with the combustion of the carbonaceous char. Optimization of furnace performance requires a better understanding of these processes occurring in the char bed.

Black liquor is fired as an aqueous solution/suspension. It is sprayed into the furnace and undergoes a number of process steps before being completely combusted. These include:

1. drying,
2. pyrolysis,
3. combustion and gasification of char,
4.  $\text{Na}_2\text{S}$  formation.

Drying occurs when the liquor comes in contact with the hot furnace gases. In CE recovery boilers suspension drying is used. A coarse spray is employed, and the liquor particles dry in flight and then land on the char bed. B & W recovery boilers use a wall drying technique. The liquor is sprayed onto a band on the furnace walls and remains there until it dries, breaks off, and falls to the char bed.

As the dried liquor is heated further, pyrolysis occurs. During pyrolysis the organic constituents of the liquor are degraded, forming combustible gases and a carbonaceous char. The sodium organic salts in the black liquor tend to be converted to sodium carbonate. The residual products of pyrolysis -  $\text{Na}_2\text{CO}_3$ ,  $\text{Na}_2\text{SO}_4$ ,  $\text{Na}_2\text{S}$ , and carbonaceous char - are the basic constituents of the char bed.

The processes occurring on and in the char bed are critical to the performance of the recovery boiler. These include the melting of the inorganic salts so they can flow out of the furnace, the reduction of  $\text{Na}_2\text{SO}_4$  to  $\text{Na}_2\text{S}$ , and the combustion and gasification of the carbonaceous char. These processes occur simultaneously and are to some extent conflicting. In order to sort out these conflicting requirements and establish criteria for optimum performance, fundamental information on the key reactions is needed.

With these needs in mind, a project was established to study the reduction of sulfate by carbon in a molten carbonate system. It was felt that this system did fairly accurately represent the conditions which exist in a char bed, and that this

reaction represented a logical first step in a program aimed at the development of a comprehensive theory of the combustion of black liquor.

#### PROJECT OBJECTIVES

The basic objectives of this project were to obtain fundamental kinetic data on sulfate reduction with carbon, define the rate controlling process in reduction, and develop insights as to how macroscopic process variables can be controlled to improve reduction in a kraft recovery furnace. The fundamental kinetic data on sulfate reduction included studies on the effect of carbon surface area, sulfate concentration, sulfide concentration, potential catalysts, smelt composition and temperature.

Although it has been reported that sulfate reduction is dependent on the type of carbon employed as the reducing agent (1,2), there is no literature data on the effect of carbon surface area on reduction. Since the effect of carbon surface area on reduction is an essential feature in any mechanism capable of explaining sulfate reduction, one of the project objectives was to determine the dependence of reduction on carbon surface area.

Several previous studies have reported that sulfate reduction with either gaseous or solid reducing agents is an autocatalytic reaction (3,4). One of the mechanisms proposed to explain this autocatalytic behavior involves a reaction between sulfate and sulfide to form a more reactive intermediate (4,5). One of the objectives of this project was to define the autocatalytic nature of reduction with carbon and to determine the effect of sulfide on reduction.

Some of the previous studies on sulfate reduction have reported that reduction is independent of the sulfate concentration (4). To fully understand sulfate

reduction, it is necessary to define the effect of sulfate on the reduction rate and the conditions under which sulfate reduction would be independent of the sulfate concentration.

Several catalysts have been proposed for sulfate reduction with gaseous reducing agents (4,6,7). One of the objectives of this project was to determine if these catalysts have a similar effect on sulfate reduction with carbon.

Another objective was to determine the effects of temperature and melt composition on sulfate reduction. The temperature dependence of a reaction is usually incorporated into the kinetic rate expression through the use of an Arrhenius type activation energy. The magnitude of the activation energy for sulfate reduction will not only define the temperature dependence, but will also aid in determining if reduction is mass transfer or kinetically controlled.

Since reoxidation of sulfide occurs in a recovery furnace, the oxidation rate of sulfide relative to the reduction rate of sulfate is important in defining the controlling process parameters. Therefore, an experimental objective of this project was to determine the sulfide oxidation rate relative to reduction.

Application of this kinetic data to the operation and control of a recovery furnace requires the development of mechanisms and rate expressions based on this data. Rate expressions based on the actual reactions occurring during reduction will aid in the development of insights into the processes controlling sulfate reduction in a kraft recovery furnace.

The final objective in this phase of the work was to take the kinetic model developed in the study and apply it to the interpretation of processes occurring in

the char bed of a recovery furnace. It provides a unifying structure for interpreting existing data on char beds, suggests furnace parameters which are important for overall reduction efficiency, and sheds light on the nature of char combustion.

## SULFATE REDUCTION CHEMISTRY

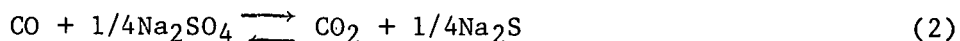
### BASIC CHEMISTRY

The reduction of sodium sulfate to sulfide can be written as:



The basic step in reduction is removal of oxygen from sulfur. However, due to unfavorable equilibrium this reaction will not proceed as written. For this reaction to proceed, a reducing agent must be present to bind with and remove the oxygens from the sulfur. The fundamental requirement of this reducing agent is that it have a greater affinity for oxygen than sulfide has for oxygen.

An indication of the strength of the reducing environment required to reduce sulfate can be gained from studying the equilibrium of the following reaction.



If we consider this reaction to be between gases and a condensed phase and these gases to be ideal, the equilibrium constant for this reaction can be written as:

$$K_p = P_{\text{CO}_2}/P_{\text{CO}} \quad (3)$$

Where  $P_{\text{CO}_2}$  is the partial pressure of  $\text{CO}_2$

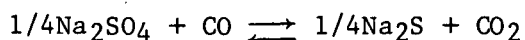
$P_{\text{CO}}$  is the partial pressure of  $\text{CO}$

Since  $\text{CO}$  is a reducing gas and  $\text{CO}_2$  is a fully oxidized species, this equilibrium ratio indicates the strength of the reducing environment required for

sulfate reduction. Table I contains the equilibrium ratio of  $\text{CO}_2/\text{CO}$  for this reaction. At the bed temperature of a recovery furnace, the equilibrium ratio of  $\text{CO}_2/\text{CO}$  is approximately 20, indicating that only a mild reducing environment is required for sulfate reduction.

TABLE I

EQUILIBRIUM  $\text{CO}_2/\text{CO}$  RATIOS



$\text{CO}_2/\text{CO}$	100	35.5	18.8	8.4
Temp., °F	980	1340	1700	2240

The principal reducing agents found in a recovery furnace are hydrogen, carbon monoxide, and carbon. Table II illustrates the various reduction reactions for sulfate in the presence of these reducing agents plus the oxidation of sulfide and the heat of reaction.

TABLE II

REDUCTION REACTIONS OF SODIUM SULFATE

Reaction	$\Delta H$ , heat of reaction	Btu/lb $\text{Na}_2\text{SO}_4$
Temperature	1340°F	1880°F
$\text{Na}_2\text{SO}_4 + 2\text{C} \rightarrow 2\text{CO}_2 + \text{Na}_2\text{S}$	542	506
$\text{Na}_2\text{SO}_4 + 4\text{C} \rightarrow 4\text{CO} + \text{Na}_2\text{S}$	1576	1521
$\text{Na}_2\text{SO}_4 + 4\text{CO} \rightarrow 4\text{CO}_2 + \text{Na}_2\text{S}$	-491	-509
$\text{Na}_2\text{SO}_4 + 4\text{H}_2 \rightarrow 4\text{H}_2\text{O} + \text{Na}_2\text{S}$	-70	-122
$\text{Na}_2\text{S} + 2\text{O}_2 \rightarrow \text{Na}_2\text{SO}_4$	-2934	-2901

Although all these reactions may be occurring in a recovery furnace, the fundamental reducing agent is carbon, and reduction in a recovery furnace is an



endothermic reaction. Reoxidation of sulfide, which occurs in the oxidizing environment at the bed's surface and in the smelt stream from the recovery furnace, is a highly exothermic reaction.

#### PREVIOUS WORK

One of the earliest studies on sulfate reduction was conducted by Budnikoff and Shilov (6) using carbon monoxide, hydrogen, and carbon as reducing agents. Their experimental technique consisted of heating a platinum boat containing sodium sulfate in an electric furnace while purging the system with either inert or reducing gases. The sample was then removed from the furnace and analyzed for sulfide and sulfate.

One of the more interesting results from this study was that at 850°C or below carbon would not reduce sulfate under an inert atmosphere. However, when either carbon monoxide or dioxide were used as the purge gas, the sulfate was reduced with yields of 80% sulfide being obtained in less than an hour at 850°C.

This result suggests that reduction of sulfate with carbon under the conditions of this study involves a carbon monoxide-dioxide cycle as shown in Eq. (4) and (5).

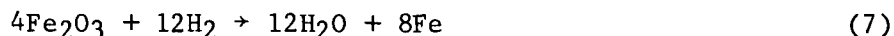
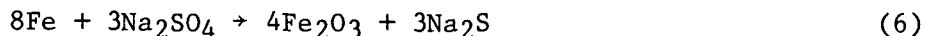


Here, carbon monoxide is oxidized by sulfate Eq. (4) to form sulfide and carbon dioxide. The carbon dioxide is then reduced by carbon Eq. (5) to form additional carbon monoxide.

In addition to the work of Budnikoff and Shilov (6), several studies have been conducted on sulfate reduction using a variety of reducing agents. With carbon as the reducing agent, the rate of reduction is strongly dependent on the nature of the carbon. White and White (1) determined that coal and charcoal had the greatest reactivity followed by lampblack and Acheson graphite, respectively.

With gaseous reducing agents, Nyman and O'Brien (7) determined that  $H_2$  was the most effective, followed by  $H_2S$ ,  $NH_3$ , and  $CH_4$ , respectively. Budnikoff and Shilov (6) reported that the reactivity of  $H_2$  was much greater than that of  $CO$ .

Several authors have reported that certain metals will catalyze the reduction of sodium sulfate. Iron has been found to be the most effective catalyst with hydrogen as the reducing agent. The catalytic effect of iron was clearly demonstrated in the work of Nyman and O'Brien (7) and later confirmed by Birk *et al.* (4). Nyman and O'Brien (7) also reported that copper(II) sulfate was an effective catalyst when hydrogen was used as the reducing agent. The following mechanism has been proposed for the catalytic effect of iron in sulfate reduction when  $H_2$  is used as the reducing agent.



Here, elemental iron reduces sodium sulfate to form sodium sulfide and ferric oxide; the ferric oxide is in turn reduced by hydrogen, reforming elemental iron.

Budnikoff and Shilov (6) reported that carbon catalyzes sulfate reduction in the presence of carbon monoxide, and Kunin and Kirillov (8) reported that carbon catalyzes sulfate reduction in the presence of hydrogen. The work of Kunin and

Kirillov (8) indicated an apparent 25% increase in the reduction rate with a small amount of lampblack present. Although this indicates some catalytic effect of carbon, this increase in rate is small compared to the effect of iron.

Sulfate reduction has been found to be autocatalytic with both gaseous and solid reducing agents (3,4). Birk et al. (4) demonstrated that a large initial amount of sulfide increased the initial reduction rate for sulfate from 28% per hour without sulfide present to 37% per hour. Birk et al. (4) proposed that the catalytic nature of sulfide was due to a reaction between sulfide and sulfate to form a more reactive intermediate. It is also possible that the autocatalytic nature of sulfate reduction may be due to an increase in the oxidized product, water in the case of hydrogen as the reducing agent, carbon dioxide in the case of carbon monoxide, and carbon monoxide/dioxide in the case of carbon.

Birk et al. (4) reported that the reduction of sulfate with hydrogen is zero order in sulfate. Nyman and O'Brien (7) presented data indicating that sulfate reduction by hydrogen without iron present was independent of sulfate until approximately 90% of the sulfate was reduced. At this point, the reduction rate decreased indicating the dependence of reduction on sulfate concentration. The determination of the reduction rate dependence on sulfate is complicated by the autocatalytic nature of the reaction. As reduction proceeds, the increase in the rate due to the reaction's autocatalytic behavior is greater than the decrease in rate due to the depletion of sulfate. However, once the sulfate is reduced to a low level, its effect should be observed and the reaction rate should decrease.

## EXPERIMENTAL SYSTEM

In a kraft recovery furnace, sulfate reduction occurs in a melt consisting principally of sodium sulfate, sodium sulfide, sodium carbonate, and carbonaceous char. To obtain kinetic data on sulfate reduction, an experimental system was designed to monitor sulfate reduction in an environment similar to that found in a kraft recovery furnace.

Figure 1 illustrates the experimental system employed to study the reduction of sodium sulfate in the presence of carbon. The reaction vessel consists of an alumina crucible contained in an electric furnace. The reduction reaction was followed by measuring the evolution of carbon monoxide and carbon dioxide, which were removed from the reactor with a nitrogen purge stream. Knowing the nitrogen purge rate to the reactor and the percentages of carbon monoxide and carbon dioxide in the purge stream from the reactor allowed the rate of sulfate reduction to be determined.

To accurately measure the volumetric flow rate of the nitrogen purge stream, the nitrogen was metered from a pressurized gas cylinder through a dry gas meter. Next the purge stream passed through an orifice meter which gave a direct reading of the flow rate and enabled approximate adjustments to be made in the flow rate. Before the purge stream entered the reactor, its temperature was measured with a thermocouple. A mercury manometer connected to the purge line served as a pressure release valve. If the purge line from the reactor became plugged, this manometer would blow, releasing the purge pressure and preventing over pressurization of the reactor.

The nitrogen purge stream plus any carbon dioxide and carbon monoxide generated by the reaction was conveyed from the reactor in a 1/4-inch steel tube.

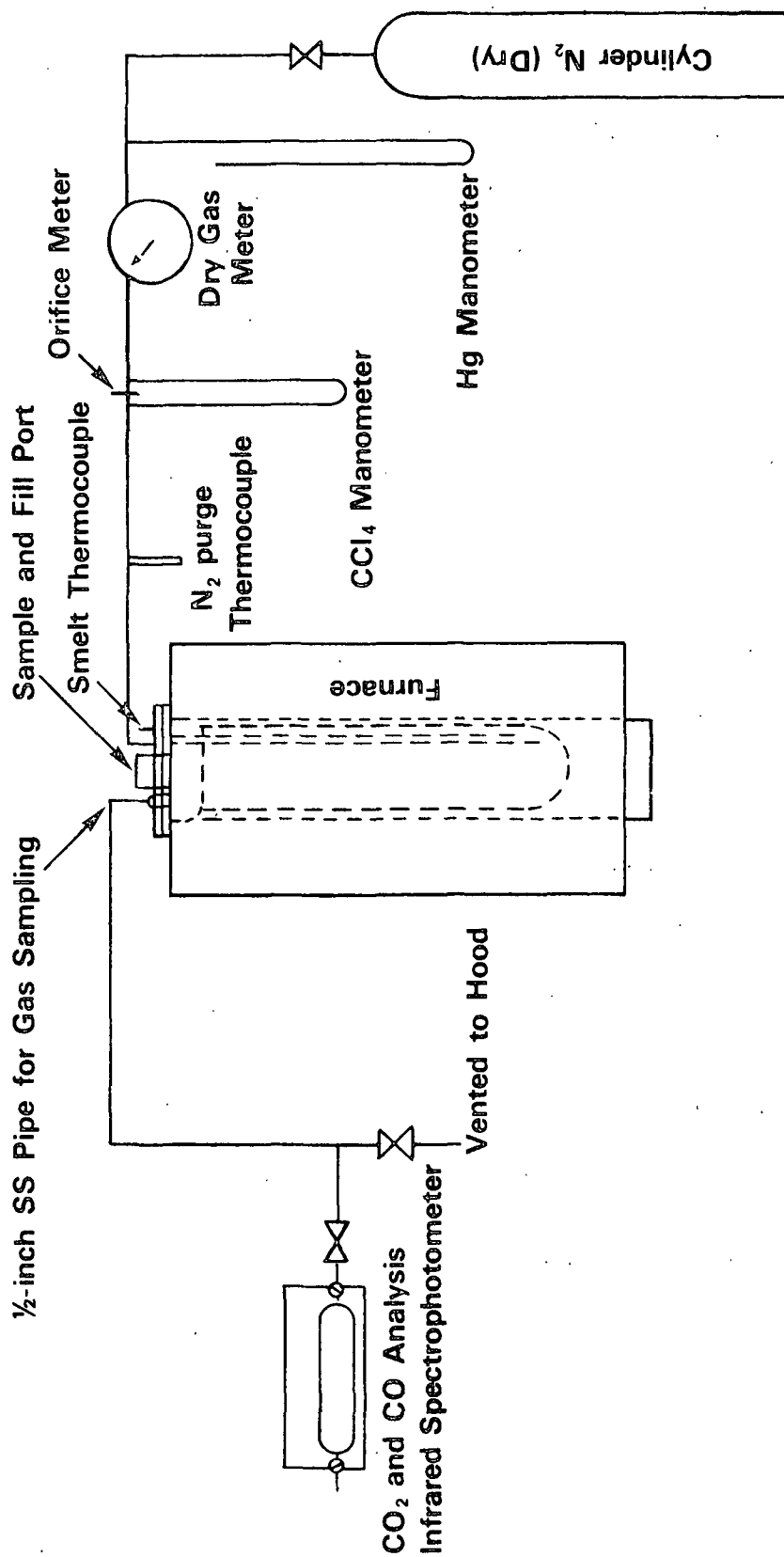


Figure 1.. Experimental System

This gas stream then passed through a filter to remove any particles and to a carbon monoxide-carbon dioxide infrared gas analyzer.\* The infrared analyzer was capable of simultaneously measuring both carbon monoxide and carbon dioxide over a 0 to 30% range. Before each experimental run, the infrared analyzer was calibrated using a standard carbon dioxide, carbon monoxide and nitrogen mixture. Checking the calibration after each run indicated that the infrared system was very stable during the reduction runs.

Figure 2 illustrates the alumina crucible-electric furnace section of the reactor system. The cylindrical crucible has an inside diameter of 4-1/8 inches, a wall thickness of 1/4-inch, and a height of 18 inches. During a typical reduction run, the crucible would contain approximately 3000 grams of smelt occupying 1.5 liters.

A steel retort 1/8-inch in diameter was located between the alumina crucible and electric furnace. If a leak developed in the alumina crucible, the smelt would be contained by this steel retort, protecting the furnace from corrosive attack. When the furnace was operating, both sides of the retort were swept with nitrogen to prevent oxidation of the retort. However, to avoid any unknown dilution of the gas sample from the reactor, the nitrogen purge to the interior of the steel retort was discontinued during a reduction run.

The nitrogen purge gas entered the reactor through an 1/8-inch inside diameter alumina tube with the open end located 1 to 2 inches from the bottom of the crucible. This ensured that the carbon and smelt were well mixed and helped strip the carbon monoxide and carbon dioxide from the smelt.

---

\*Model IR 702/703, Infrared Industries, Inc., Santa Barbara, California.

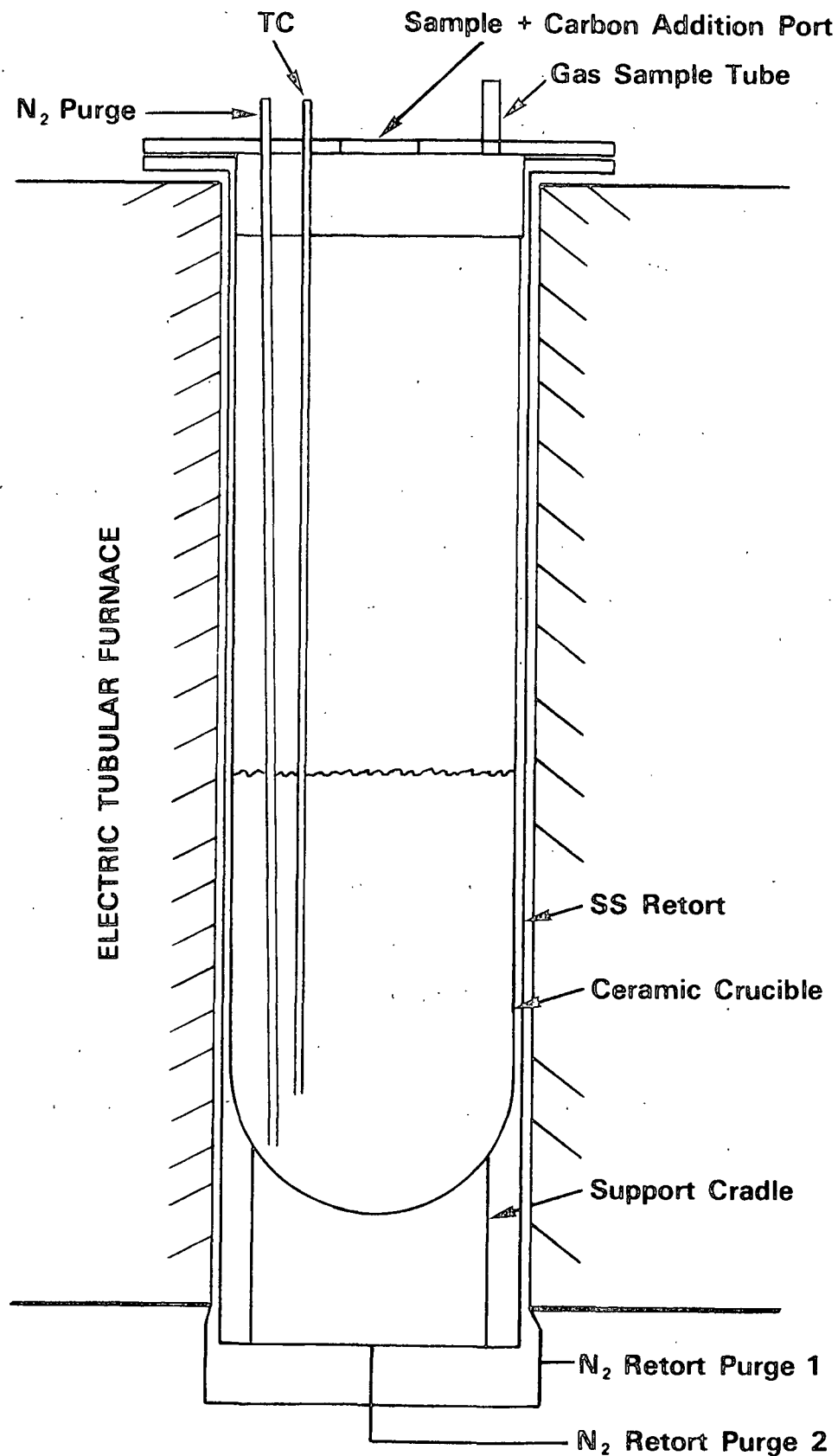


Figure 2. Experimental Reactor

A chromel-alumel thermocouple was used to monitor smelt temperature. The smelt temperature was maintained at the desired temperature using an on-off temperature controller to regulate furnace temperature.

To prepare for a reduction run, anhydrous, reagent grade alkali carbonates and sodium sulfate were premixed and added to the alumina crucible. A typical charge consisted of 25 moles of sodium carbonate and 1 mole of sodium sulfate. This ratio of sodium sulfate to sodium carbonate produced a reduction rate that was easily monitored. Also, considering the sodium sulfide present as inert, the mole ratio of sulfate to inerts in a recovery furnace is close to the ratio used here. To prevent damage to the furnace, the temperature of the system was slowly increased until a temperature a few degrees above the desired reduction run temperature was reached. The reduction reaction was then initiated by adding carbon rods 1-inch in length and either 1/8- or 3/8-inch in diameter to the smelt. The carbon rods used were a mixture of amorphous carbon and graphite manufactured by Becker Brothers Carbon Corporation, Cicero, Illinois. Once the carbon rods were added, the reactor was sealed and the nitrogen purge to the reactor started. The reaction was then followed through the evolution of carbon monoxide and carbon dioxide. The reactor design also allowed smelt samples to be removed from the reactor during a run. These samples could be analyzed for sulfate and sulfide and the extent of reduction compared to that predicted through carbon monoxide and carbon dioxide evolution.



## EXPERIMENTAL RESULTS

One of the principal objectives of this study was to determine the effects of the following parameters on sulfate reduction: a) carbon loading and carbon surface area, b) sulfate concentration, c) sulfide concentration, d) temperature, e) catalysts, and f) smelt composition. The study of these parameters is necessary to understand the nature of sulfate reduction. The experimental results obtained during the study of these parameters are contained in this section.

Since carbon monoxide is present in large quantities in a recovery furnace and will also reduce sodium sulfate, a brief study was made on sulfate reduction with carbon monoxide. Anytime the reduced smelt in a recovery furnace contacts air, oxidation of the sulfide will occur. Therefore, another brief study was made on oxidation of sulfide. The experimental results of these two studies are also contained in this section.

Birk et al. (4) determined that sulfate reduction with hydrogen could be accurately described with a rate expression of the following form:

$$\frac{d[\text{SO}_4]}{dt} = - K_1 [\text{P}_{\text{H}_2}]^a [\text{S}^-]^b [1 + K_2 [\text{Fe}]^c] \quad (8)$$

where  $\frac{d[\text{SO}_4]}{dt}$  is the change of sulfate concentration with time,

$K_1$  is the overall rate constant,

$[\text{P}_{\text{H}_2}]$  is the partial pressure of  $\text{H}_2$ ,

$[\text{S}^-]$  is the sulfide concentration,

$K_2$  is the rate constant for iron catalyzed reduction,

$[\text{Fe}]$  is the iron concentration.

The initial approach taken in the study of sulfate reduction with carbon was to determine if a similar expression could be developed to describe sulfate reduction with carbon. Such a rate expression is shown below:

$$\frac{d[\text{SO}_4]}{dt} = - K_1 [\text{SO}_4^-]^a [\text{S}^-]^b [\text{CSA}]^c [1 + K_2 [\text{Fe}]^d] \quad (9)$$

where  $[\text{SO}_4^-]$  is the sulfate concentration,  
 $[\text{CSA}]$  is the carbon surface area.

Rates of carbon monoxide and carbon dioxide generation and sulfate reduction obtained during a typical reduction experiment are shown in Fig. 3. Although the reduction rates vary, dependent on the initial level of reagents and temperature of the system, the basic shape of this reduction curve is representative of the sulfate reduction rates seen in this study.

As illustrated in Fig. 3, sulfate reduction with carbon is a highly autocatalytic reaction. The reaction begins with an induction period of about 6 minutes, followed by a sharp rate increase, a peak and, depending on the reaction parameters, either a gradual or sharp rate decrease.

#### CARBON SURFACE AREA EFFECT

Since carbon is the reducing agent, the reduction rate should be highly dependent on the amount of carbon surface area available and the type of carbon used. The experimental objective in terms of carbon was to determine the effect of carbon surface and carbon loading on the sulfate reduction rate.

A few initial reduction experiments were conducted with activated granular carbon. Here, reduction occurred so rapidly that the reaction was difficult to follow. Therefore, amorphous carbon-graphite rods were chosen as the source of

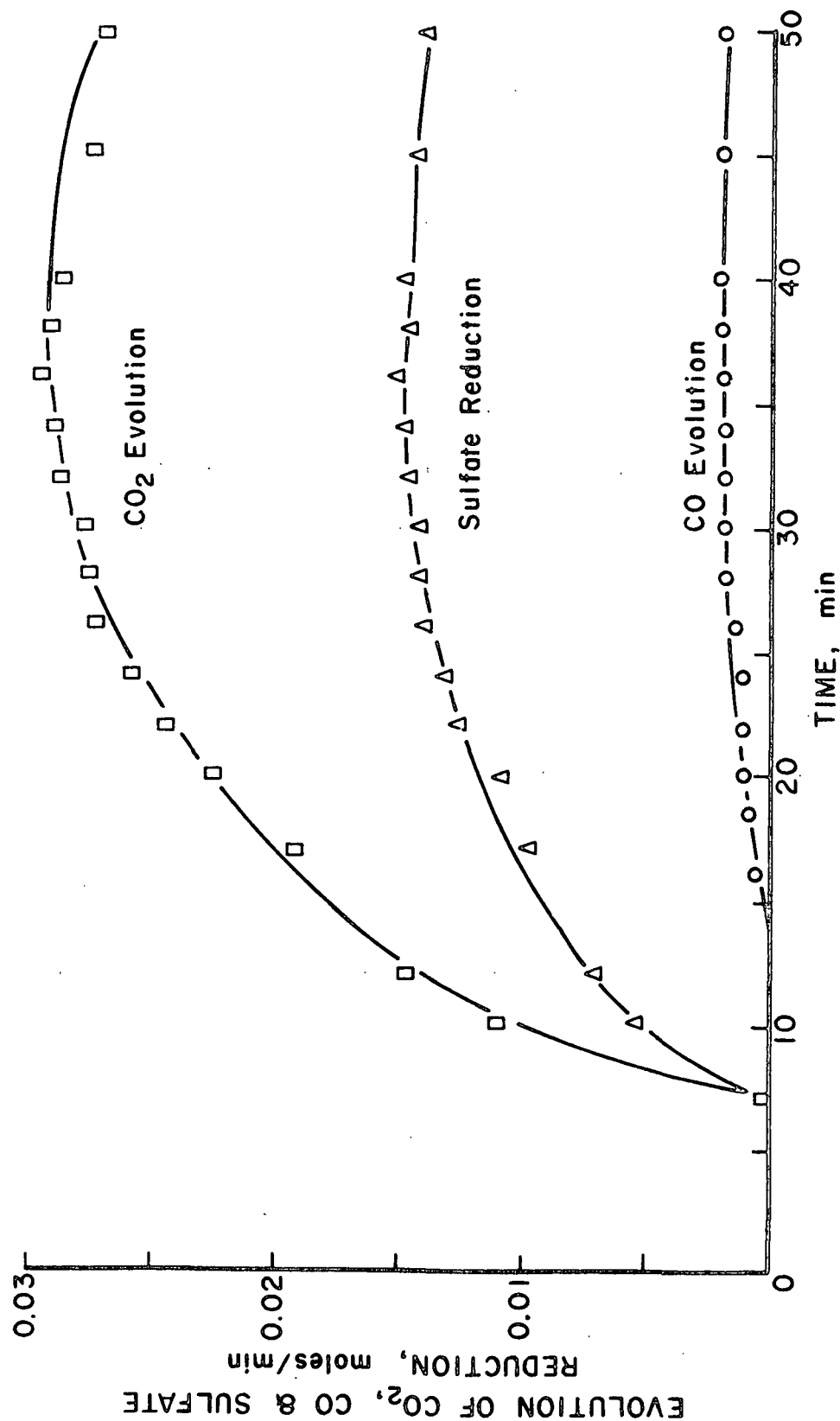


Figure 3. Sulfate Reduction with Carbon

carbon. These rods allowed the carbon surface area to be readily calculated and were easily dispersed in the smelt.

To determine the effect of carbon surface area on reduction rate, several reduction runs were made using different levels of carbon. Both 3/8-inch and 1/8-inch rods were used for these experiments.

The effect of carbon surface area on reduction rate is shown in Fig. 4. The carbon surface area was calculated assuming that the shrinkage of the carbon rods during the reaction was uniform. Each reduction experiment in Fig. 4 initially had 1.0 mole of sulfate present, and the reaction rate was measured with 0.2 mole of sulfate converted to sulfide. This ensured that the reaction rates in Fig. 4 were measured with the same amount of sulfate and sulfide present.

Since Fig. 4 is a plot of log (reaction rate) vs. log (carbon surface area), the slope of this curve is the reaction order with respect to carbon surface area. A least squares fit of this curve yields a slope of  $0.50 \pm 0.06$ . Therefore, the sulfate reduction is proportional to the square root of the carbon surface area.

At 0.2 mole of sulfate converted to sulfide, the reaction rate is 70% to 80% of the maximum rate, and the carbon surface area is close to the initial surface area. Therefore, a plot of log (maximum rate) vs. log (initial carbon surface area) would yield results similar to those obtained from Fig. 4.

In addition to the square root dependence of rate on carbon surface area, the reaction rate is dependent on the type of carbon used. Carbon rods obtained from the supplier at different times varied up to 20% in their reactivity. Apparently, the number of active sites on the carbon rods varied with small changes in composition or manufacturing conditions.

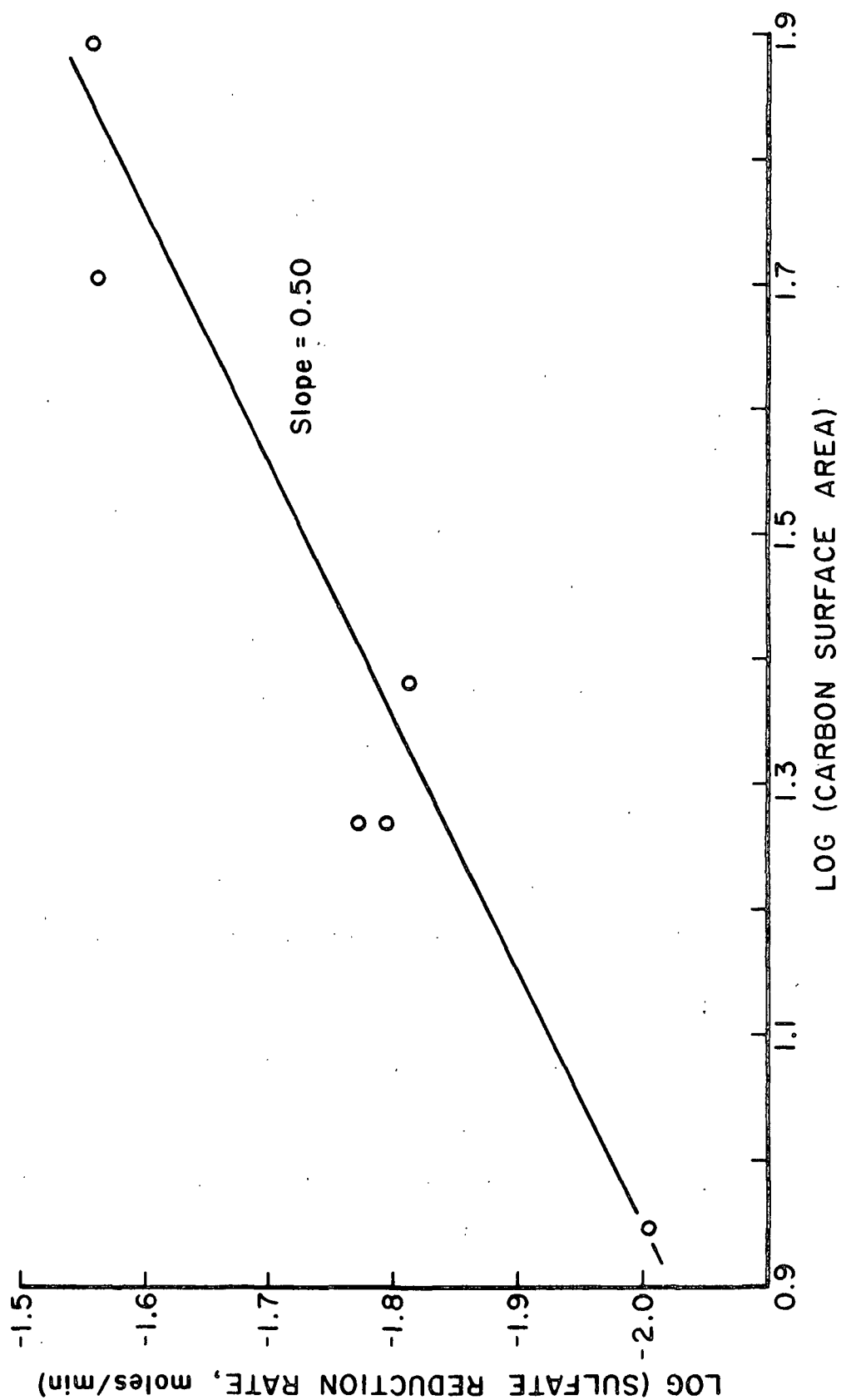


Figure 4. Effect of Carbon Surface Area on Sulfate Reduction with Carbon

## SULFATE EFFECT

The approach used to determine the sulfate effect on reaction rate was similar to that used with carbon. The amount of sulfate added to the smelt varied from 0.25 to 3.5 moles.

Figure 5 illustrates the effect of sulfate on the rate of sulfate reduction. The reaction rates in Fig. 5 were determined with 0.1 mole of sulfate converted to sulfide. This ensured that each rate was determined with the same level of sulfide and carbon surface area present.

As seen in Fig. 5, sulfate reduction with carbon varies from first order in sulfate at low sulfate concentrations to zero order in sulfate at high sulfate concentrations. The break in the curve should be dependent on the type of carbon used. A more porous or active carbon should raise the level of sulfate required to produce a reaction rate that is zero order in sulfate.

A literature review did not reveal any previous reports of sulfate reduction being first order in sulfate with either gaseous or solid reducing agents. However, Birk et al. (4) reported that sodium sulfate reduction with hydrogen was zero order in sulfate.

One explanation for the effect of sulfate is that reduction with carbon involves a series of simultaneous reactions. At low levels of sulfate, the reaction involving sulfate is rate limiting and at high levels of sulfate another of the reactions in the series is rate limiting.

## SULFIDE EFFECT

With hydrogen as the reducing agent, Birk et al. (4) reported that the autocatalytic nature of sulfate reduction resulted from the increase in sulfide as

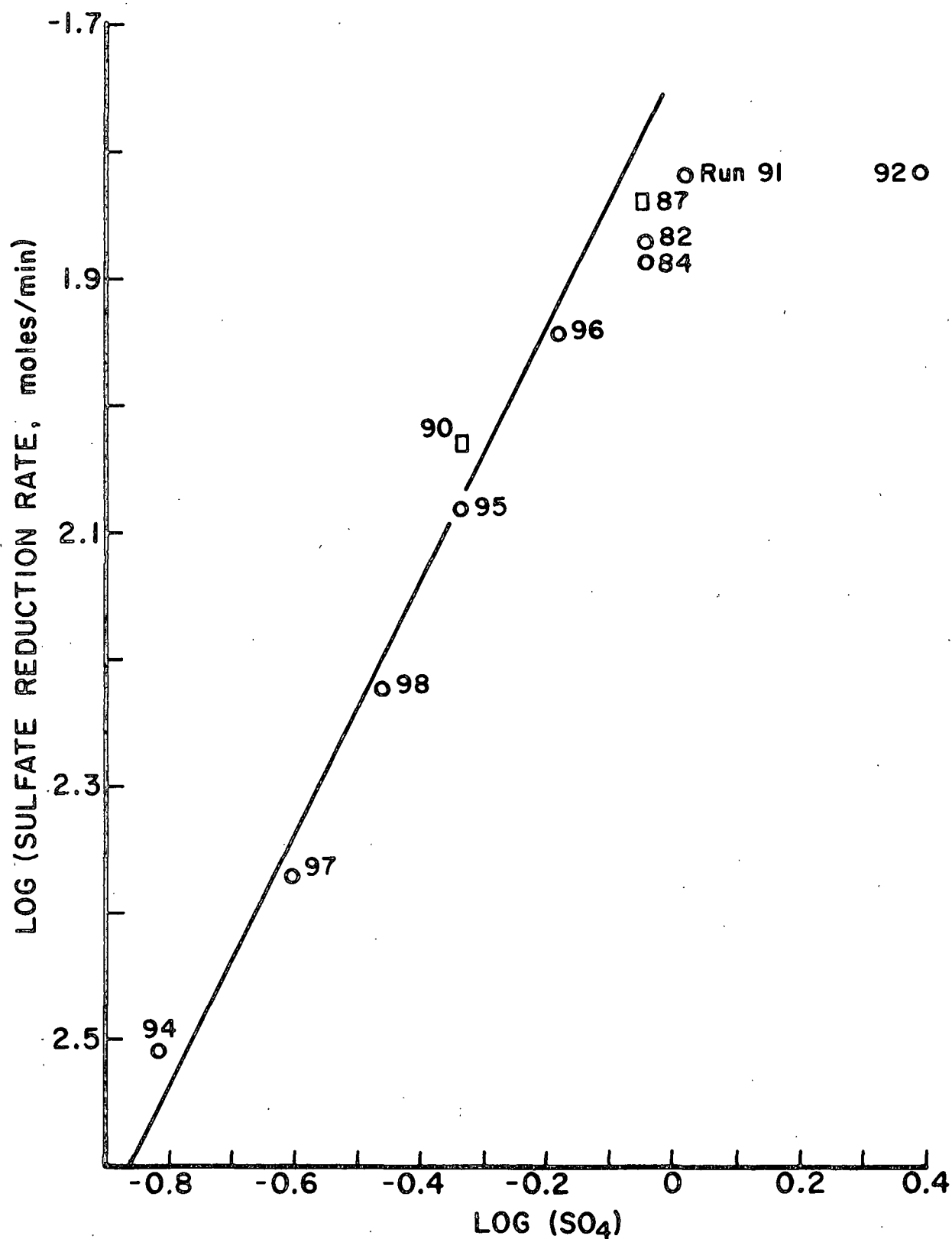


Figure 5. Effect of Sulfate on Sulfate Reduction with Carbon

the reaction proceeded. To determine if sulfide could account for the autocatalytic nature of sulfate reduction with carbon, several reduction experiments were conducted with initial amounts of sulfide added. Two of these experiments with initial levels of sulfide are Runs 87 and 90 in Fig. 5.

Anhydrous sodium sulfide was prepared by dehydrating crystallized  $\text{Na}_2\text{S} \cdot 9\text{H}_2\text{O}$  under a nitrogen atmosphere at  $180^\circ\text{C}$ . Laboratory analysis of anhydrous sulfide prepared in this manner determined that the samples contained 95 to 97% sulfide and 1 to 2% sulfate.

Sulfate reduction with initial sulfide present indicates that sulfide has no effect on the sulfate reduction rate. Although Runs 87 and 90 have initial amounts of sulfide present, their reduction rates fall on the same curve in Fig. 5 as the runs with no initial sulfide present. Figure 6 is the reduction rate curve for Run 90 and illustrates that the shape of the reduction curve is not affected by the addition of relatively large initial levels of sulfide.

#### IRON CATALYST EFFECT

Various transition metals have been shown to catalyze sodium sulfate reduction with hydrogen or carbon monoxide. For sulfate reduction with hydrogen, iron in the form of  $\text{FeSO}_4$  or  $\text{Fe}_2\text{O}_3$  was the most effective catalyst (4).

If the mechanism of sulfate reduction with carbon is similar to that with carbon monoxide or hydrogen, iron should also catalyze sulfate reduction with carbon. To determine the effect of iron on sulfate reduction with carbon, several reduction experiments were conducted with various levels of  $\text{FeSO}_4$  present.

The effect of iron on sulfate reduction with carbon was studied at different temperatures and smelt compositions. Figure 7 is representative of the



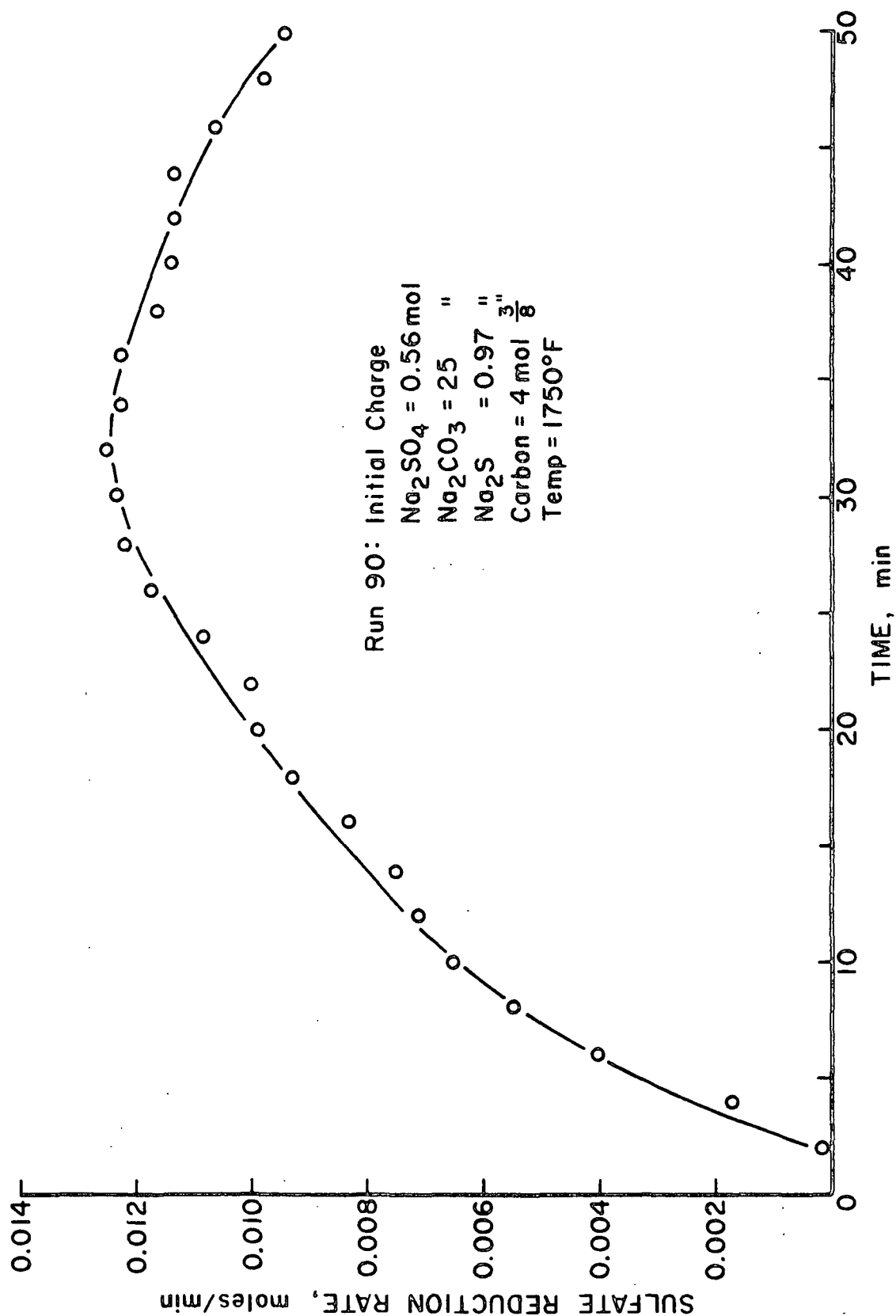


Figure 6. Effect of Sulfide on Sulfate Reduction with Carbon

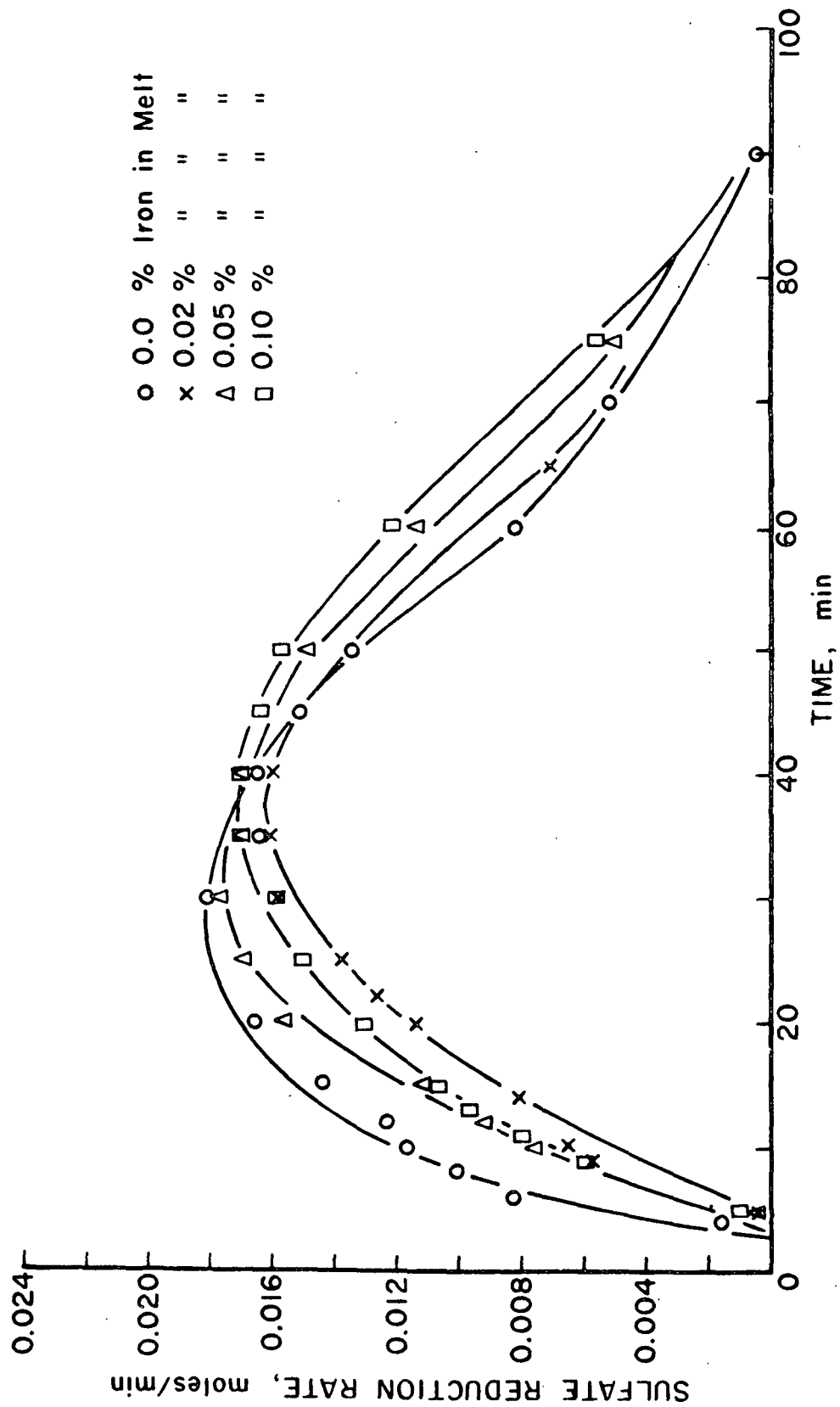


Figure 7. Effect of Iron on Sulfate Reduction with Carbon

results of these experiments. Here, the rates of reduction at 1750°F in  $\text{Na}_2\text{CO}_3$  are shown with different amounts of iron added. The shape of these curves demonstrates that iron has no effect on sulfate reduction with carbon. The slight differences in the reduction rates shown in Fig. 7 are principally due to temperature variations during the reaction.

#### TEMPERATURE AND MELT COMPOSITION EFFECTS

To determine the effect of temperature, sulfate reduction was studied over a temperature range of 1500°F to 1800°F. Due to freezing of the melt, 1650°F was the lowest temperature at which sulfate reduction in a melt consisting primarily of  $\text{Na}_2\text{CO}_3$  was studied. To study reduction below this temperature,  $\text{Li}_2\text{CO}_3$  and  $\text{K}_2\text{CO}_3$  were added to the  $\text{Na}_2\text{CO}_3$  melt. In addition to producing lower melting point systems, the addition of  $\text{Li}_2\text{CO}_3$  and  $\text{K}_2\text{CO}_3$  enabled the effect of different melt compositions to be studied.

The temperature ranges and melt compositions studied and the calculated activation energies for reduction in these melts are shown in Table III.

TABLE III  
EFFECT OF TEMPERATURE ON SULFATE REDUCTION WITH CARBON

Runs		55-61, g moles	62-66, g moles	67-73, g moles
Melt	$\text{Na}_2\text{CO}_3$	25.0	15.0	3.61
Composition	$\text{K}_2\text{CO}_3$	0.0	10.0	7.48
	$\text{Li}_2\text{CO}_3$	0.0	0.0	13.92
	$\text{Na}_2\text{SO}_4$	1.0	1.0	1.0
	Carbon 3/8-inch	4.0	4.0	4.0
Temperature range		1650-1800°F	1600-1800°F	1500-1800°F
Activation energy		49 kcal	53 kcal	71 kcal

Sulfate reduction was found to be a highly temperature dependent reaction. Although the  $\text{Li}_2\text{CO}_3/\text{K}_2\text{CO}_3/\text{Na}_2\text{CO}_3$  melt is very fluid at  $1400^\circ\text{F}$  no reduction was observed at this temperature. Raising the reactor temperature to  $1500^\circ\text{F}$  produced only trace amounts of carbon dioxide and carbon monoxide. At  $1600^\circ\text{F}$  sulfate reduction did occur but at a very low rate.

The activation energies in Table III are based on the reduction rate at 40% of the sulfate converted to sulfide. Since the initial concentrations of reagents in Table III were the same for all runs, all the systems contained the same levels of sulfate, sulfide and carbon at 40% conversion. For the systems in Table III, the reaction rate at 40% conversion is near the maximum rate, and similar activation energies can be obtained using the maximum rate at each temperature.

The activation energies were calculated assuming that the temperature dependency can be represented by Arrhenius' Law, Eq. (10).

$$\text{Rate} = K_0 \times e^{-\Delta E/RT} \times f(\text{composition}) \quad (10)$$

where  $K_0$  is the frequency factor,

$\Delta E$  is the activation energy,

$R$  is the ideal gas constant,

$T$  is the absolute temperature,

$f(\text{composition})$  represents the composition dependent terms.

The activation energies in Table III were calculated using a least squares fit of the natural logarithm of the reduction rate, moles/minute, vs. the reciprocal of the absolute temperature,  $^\circ\text{K}^{-1}$ , as shown in Fig. 8.

The activation energy for sulfate reduction in a  $\text{Na}_2\text{CO}_3$  or  $\text{Na}_2\text{CO}_3\text{-K}_2\text{CO}_3$  melt is approximately 50 kcal. However, in  $\text{Na}_2\text{CO}_3\text{-K}_2\text{CO}_3\text{-Li}_2\text{CO}_3$  the activation

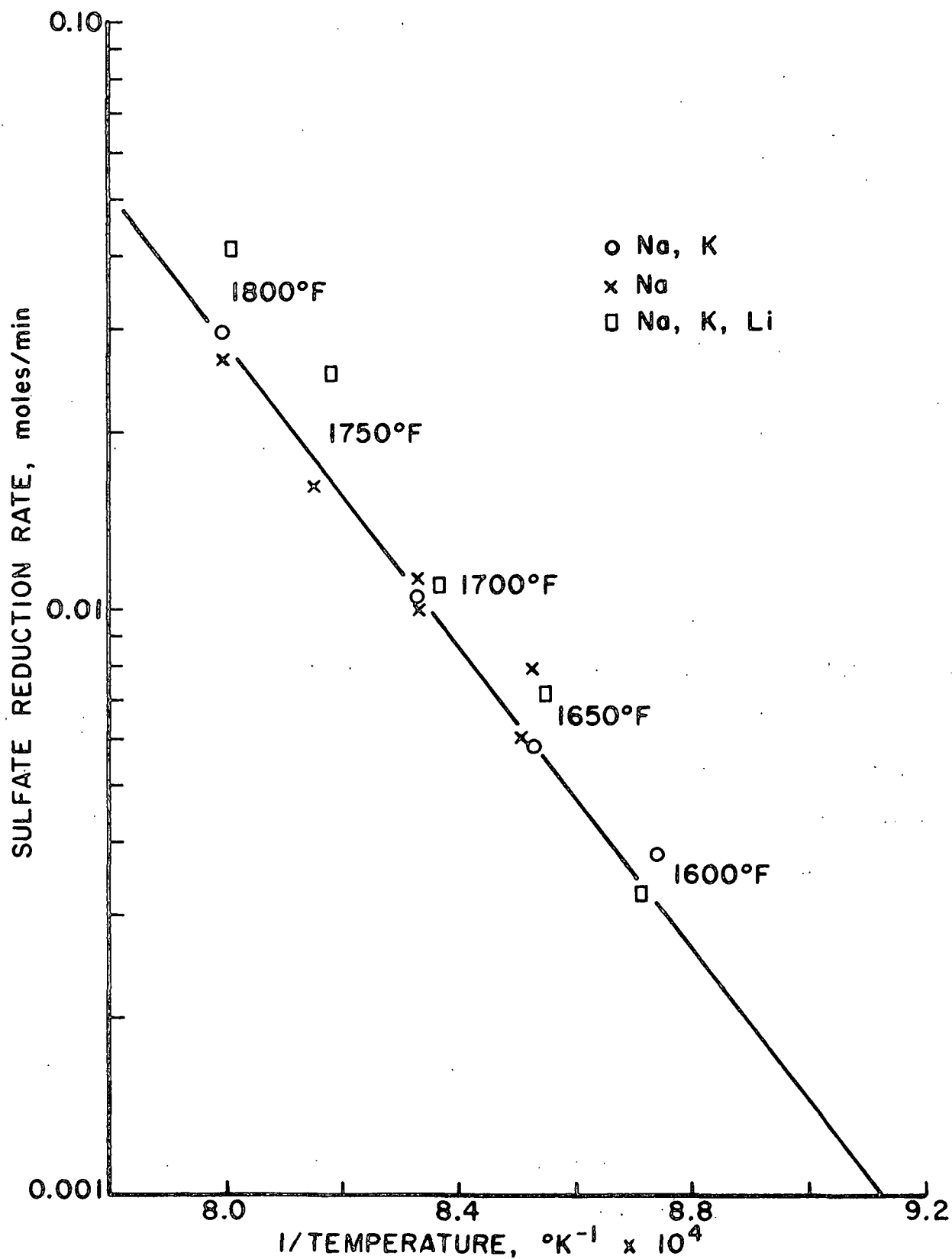


Figure 8. Effect of Temperature on Sulfate Reduction with Carbon

energy for sulfate reduction increases to 70 kcal. This difference in activation energies is evident by comparing the effect of temperature on sulfate reduction in  $\text{Na}_2\text{CO}_3$ , Fig. 9, with the effect of temperature on sulfate reduction in  $\text{Na}_2\text{CO}_3\text{-K}_2\text{CO}_3\text{-Li}_2\text{CO}_3$ , Fig. 10.

A marked difference between the melts containing only  $\text{Na}_2\text{CO}_3$  and  $\text{K}_2\text{CO}_3$  and that containing  $\text{Li}_2\text{CO}_3$  is the high level of carbon dioxide evolved from the melt before the addition of the carbon. This evolution of carbon dioxide is due to the decomposition of  $\text{Li}_2\text{CO}_3$ . Figure 11 is a plot of the partial pressure of carbon dioxide over  $\text{Li}_2\text{CO}_3$  vs. temperature. This evolution of carbon dioxide may influence reduction and account for the higher activation energy for sulfate reduction in a melt containing  $\text{Li}_2\text{CO}_3$ .

During the temperature study with the melt containing  $\text{K}_2\text{CO}_3$  an unknown compound exploded in the reactor. This compound was also deposited in the purge line from the reactor and exploded when contacted. It is suspected that this unstable compound was potassium carbonyl,  $\text{K} - \text{O} - \text{C} \equiv \text{C} - \text{O} - \text{K}$ . The literature indicates this compound may be formed when potassium salts are exposed to high temperatures and strong reducing conditions.

#### CARBON ROD TEMPERATURE EFFECT

Two separate series of experiments were conducted to determine if heat transfer to the carbon rods would account for the induction period and subsequent rapid rate increase in sulfate reduction. In one series of experiments, the carbon rods were added to the melt 15 minutes prior to the addition of sodium sulfate. Here, the reduction rate exhibited the same behavior, an induction period, rapid rate increase, peak, and decrease, as in the previous experiments.

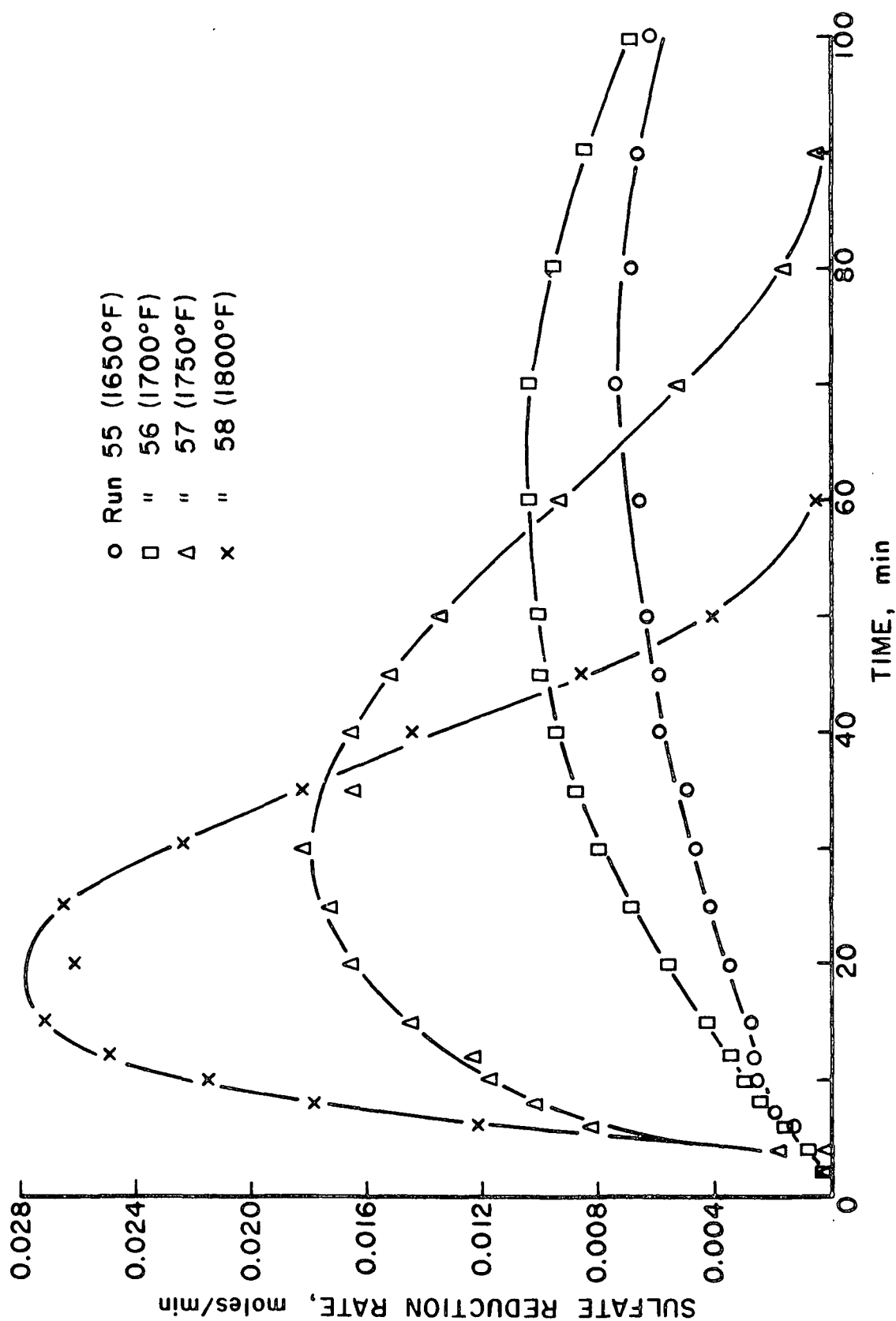


Figure 9. Effect of Temperature on Sulfate Reduction in  $\text{Na}_2\text{CO}_3$

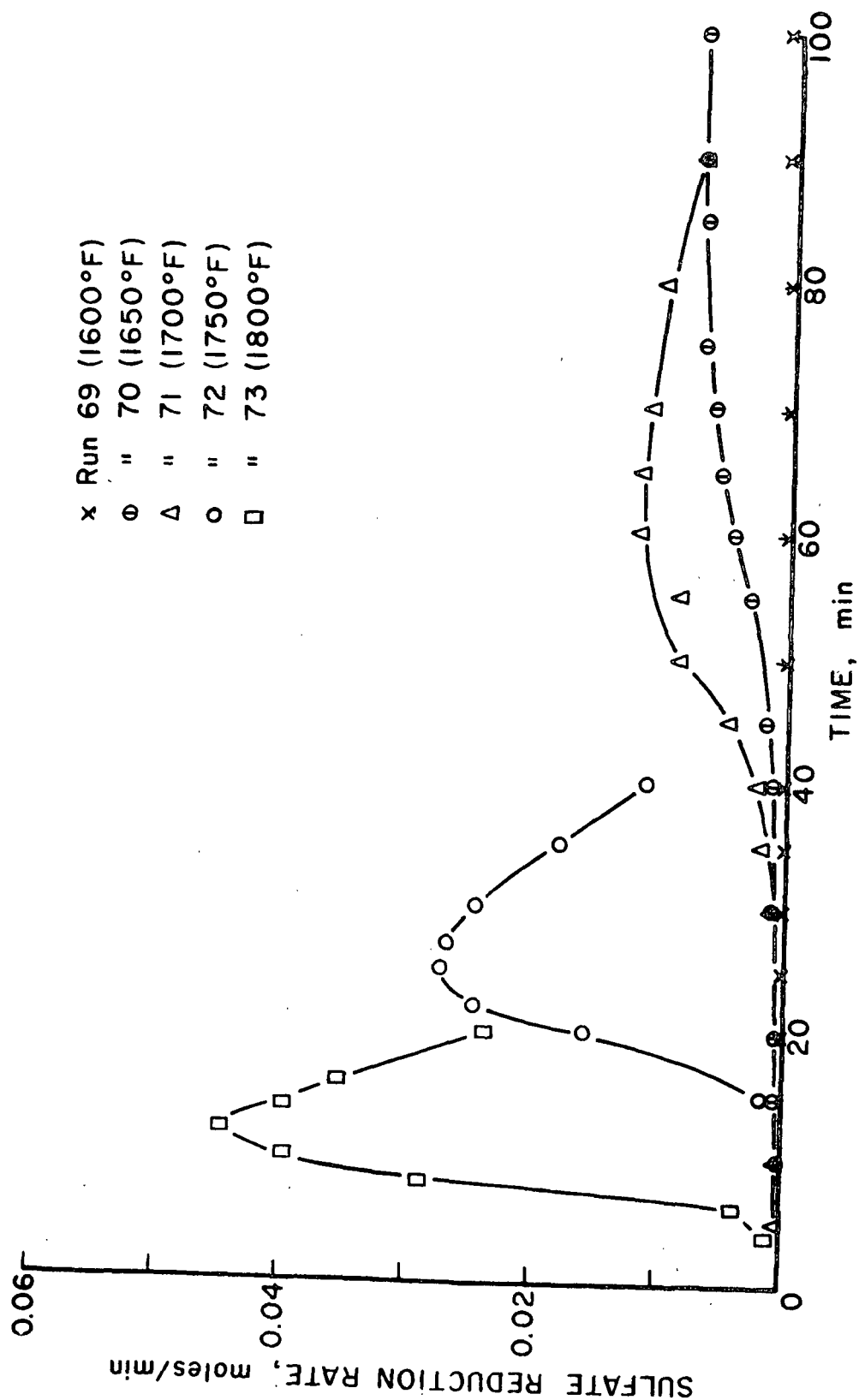


Figure 10. Effect of Temperature on Sulfite Reduction in  $\text{Na}_2\text{CO}_3\text{-K}_2\text{CO}_3\text{-Li}_2\text{CO}_3$



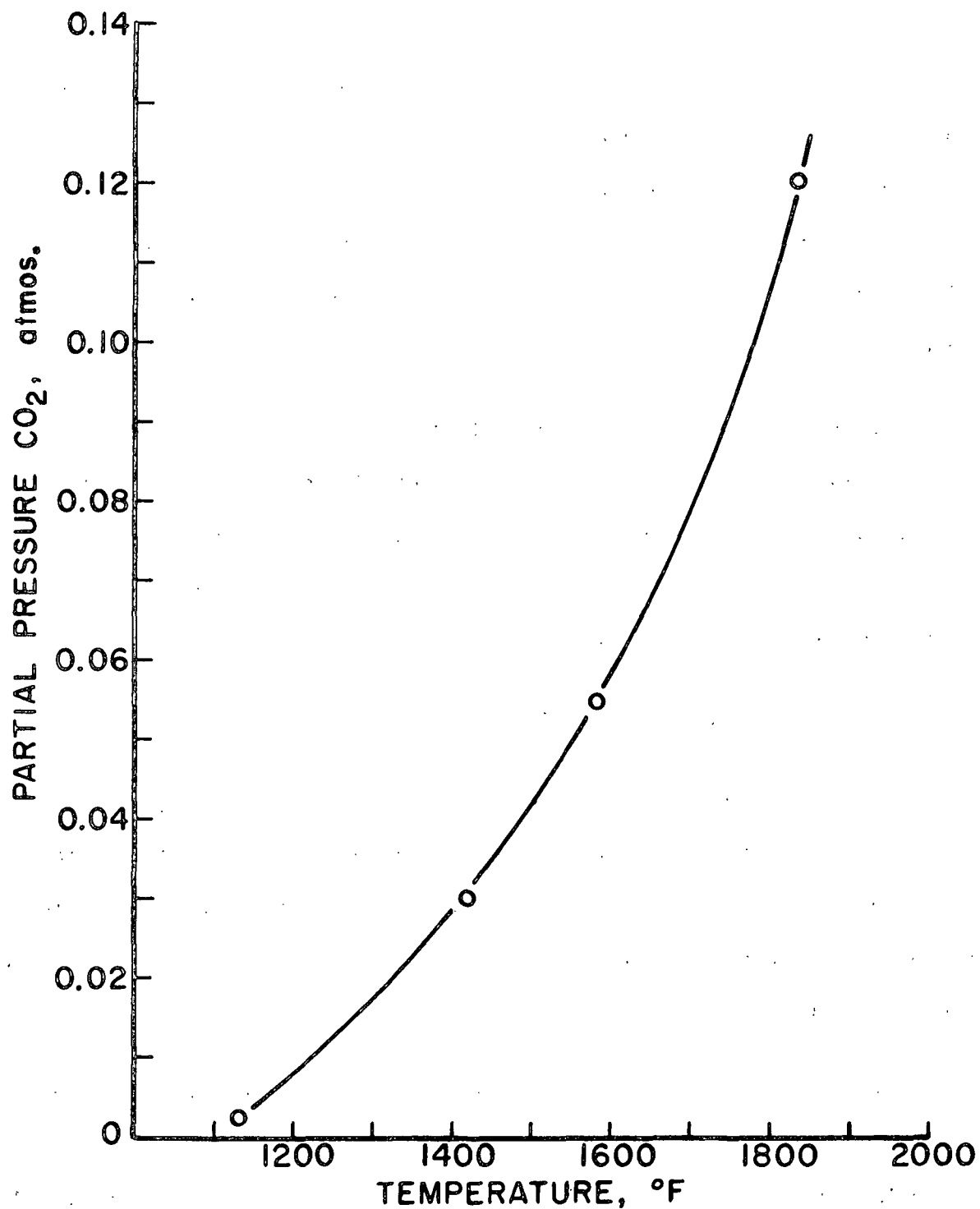


Figure 11. Partial Pressure of CO<sub>2</sub> over Li<sub>2</sub>CO<sub>3</sub>

In the second series of experiments, a hole was drilled into one end of a 12-inch-long carbon rod to within 1/8-inch of the opposite end. The rod was attached to a holder and a thermocouple inserted into the rod. This assembly was then lowered into the melt and the rod temperature followed during reduction. After 2 minutes the carbon rod was 4°F to 8°F cooler than the melt. The temperature of the rod then slowly decreased until a maximum temperature difference of 11°F to 13°F was reached.

If heat transfer to the carbon rod is the rate limiting mechanism, the reaction rate increase should follow a temperature increase in the carbon rod. Since the carbon rod temperature is initially only a few degrees cooler than the melt and decreases as the reaction proceeds, the induction period and rapid increase in rate are not due to a heat transfer limited situation.

#### SULFATE REDUCTION WITH CARBON MONOXIDE

Both carbon monoxide and carbon dioxide are evolved during the reduction of sodium sulfate with carbon. Since carbon monoxide will reduce sodium sulfate and is present in the melt, sulfate reduction with carbon monoxide occurs during reduction with carbon. Therefore, a brief study of sulfate reduction with carbon monoxide is included in this work.

To study sulfate reduction with carbon monoxide, two series of experiments were conducted with carbon monoxide added to the nitrogen purge stream. During these experiments, no carbon was added to the melt, and reduction was followed through analysis for sulfate and sulfide in melt samples.

In the first series of experiments carbon monoxide was added at 10% of the nitrogen purge; in the second series 100% carbon monoxide was used as the purge

stream. Several reduction experiments were conducted at each carbon monoxide level and the results of these experiments are shown in Table IV.

TABLE IV  
SODIUM SULFATE REDUCTION WITH CARBON MONOXIDE

Run	Purge Rate		Reduction Rate, moles Na <sub>2</sub> SO <sub>4</sub> reduced/minute	% Reduction	
				Initial	Final
4A2	5 L/min	10% CO	0.00041	0.0	0.06
4A3	5 L/min	10% CO	0.00035	0.06	0.20
4A6	5 L/min	10% CO	0.00070	0.02	0.06
5A1	5 L/min	100% CO	0.0047	0.0	6.5
5A2	5 L/min	100% CO	0.0036	0.5	9.8
5A3	5 L/min	100% CO	0.0110	9.8	24.0
5A4	5 L/min	100% CO	0.0098	23.1	31.8

The sulfate reduction rate with carbon monoxide is dependent on the amount of carbon monoxide in the melt. Better dispersion of the carbon monoxide in the melt should significantly increase the reduction rates in Table IV.

In both series of sulfate reduction experiments with carbon monoxide, 6% to 20% of the carbon monoxide supplied was consumed during the reaction. The reduction rate with 100% carbon monoxide in the purge was about 10 times as fast as the rate with 10% carbon monoxide in the purge. This indicates that reduction with carbon monoxide is proportional to the partial pressure of carbon monoxide.

#### OXIDATION OF SULFIDE

Anytime smelt in a recovery furnace is exposed to air, oxidation of sulfide occurs. The degree of sulfate reduction achieved depends not only on reduction but also on the oxidation of sulfide. Therefore, a study on the oxidation of sulfide was included in this project.

Oxidation of sulfide was studied by purging a melt containing sodium sulfide with a mixture of air and nitrogen and analyzing melt samples for sulfate and sulfide. Two different methods were employed to add sulfide to the melt. In the first method sodium sulfate was added to the melt and then reduced with carbon monoxide to yield sodium sulfide. In the second method, dehydrated sodium sulfide was added directly to the melt. Both methods of sulfide addition produced similar results on oxidation.

Figure 12 illustrates typical results obtained from the oxidation of sulfide. During this experiment, a gas purge stream containing 10% oxygen was used to oxidize the sulfide. All the oxygen supplied was consumed by the oxidation reaction. Here, the rate of oxygen addition was measured at 0.048 mole per minute and the rate of sulfide depletion at 0.026 mole per minute. The slight difference in oxygen addition and sulfide depletion was probably due to inaccuracies in the measurement of the air addition rate.

Here, the essential feature is that at the temperature range of this study, oxidation is only limited by the availability of oxygen. In comparison to reduction with either carbon or carbon monoxide, oxidation is a considerably faster reaction.

#### THIOSULFATE REDUCTION

To determine if thiosulfate reduction with carbon is similar to sulfate reduction, a series of reduction experiments using thiosulfate was conducted. At the temperature range of the study, thiosulfate is unstable and could not be premixed with the sodium carbonate and melted as was done with sodium sulfate. Since the thiosulfate could not be premixed with the sodium carbonate and pure sodium carbonate has a relatively high melting point, a small amount of lithium carbonate was

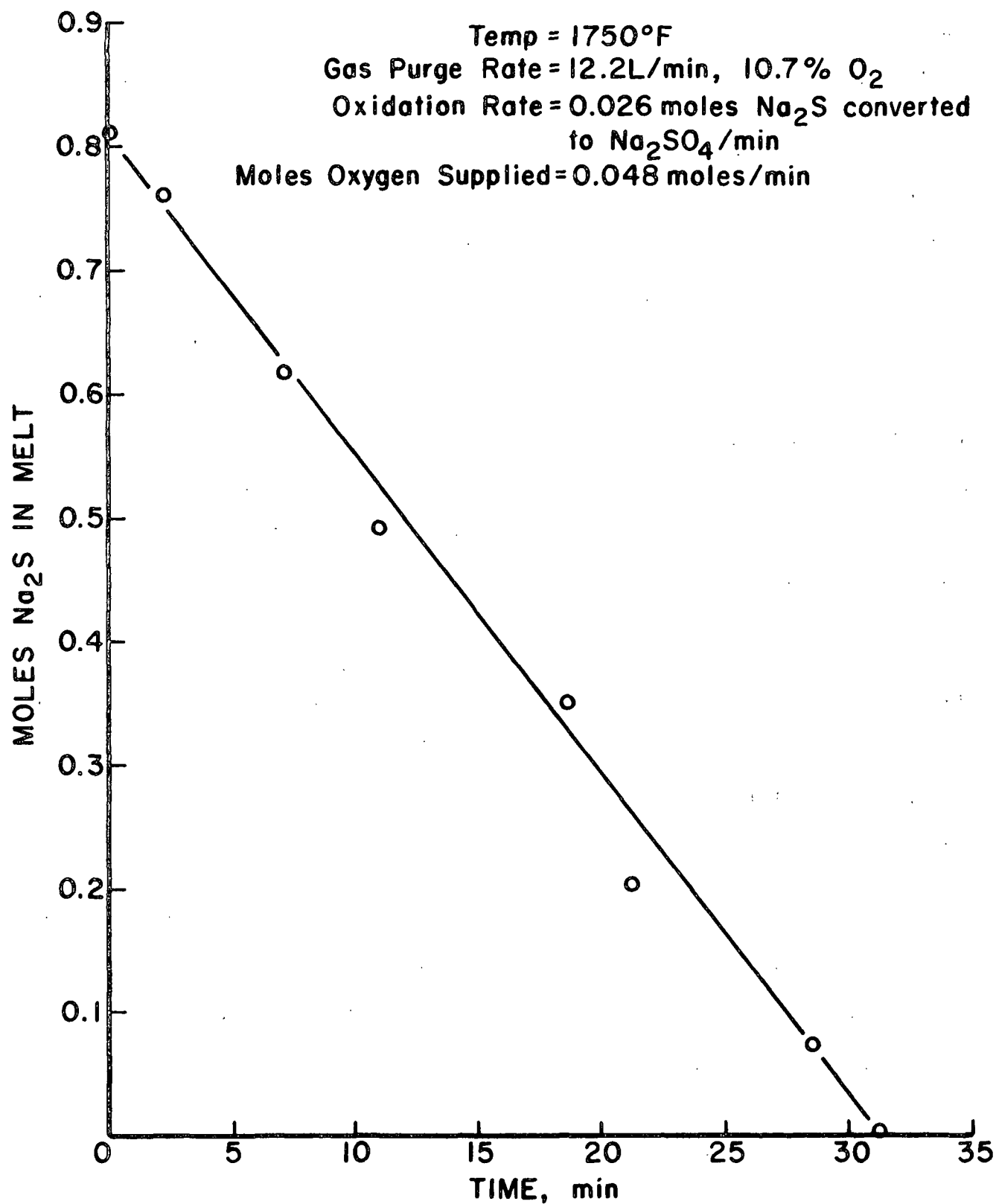


Figure 12. Oxidation of Sodium Sulfide

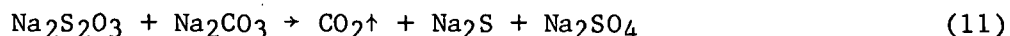
added to lower the system's melting point. Thiosulfate was added to this  $\text{Li}_2\text{CO}_3$ - $\text{Na}_2\text{CO}_3$  melt at  $1850^\circ\text{F}$  and after 30 minutes the carbon rods were added to the melt.

After the addition of thiosulfate to the melt but before the addition of carbon, a considerable amount of carbon dioxide evolved from the reactor. This evolution of carbon dioxide was much greater than that obtained from the decomposition of the lithium carbonate. Once this carbon dioxide decreased to the level being evolved before the addition of the thiosulfate, approximately 30 minutes, the carbon rods were added to the reactor. Melt samples taken before the addition of the carbon rods contained approximately equal molar levels of sodium sulfate and sulfide but no thiosulfate. Once the carbon rods were added to the melt, reduction was similar to sulfate reduction. Again, the presence of sulfide did not affect the shape of the reduction rate curve.

Since the addition of thiosulfate to the reactor caused a large flare, the thiosulfate was added slowly. The total time for the addition of thiosulfate was about 5 minutes. Analysis of melt samples taken immediately after the addition of the thiosulfate indicated that only a trace amount of thiosulfate remained in the melt.

It is evident from these experiments that thiosulfate reacts with the carbonate melt to form sulfate and sulfide. Since this reaction is considerably faster than reduction at  $1850^\circ\text{F}$ , the majority of the thiosulfate is converted to sulfate and sulfide before reduction begins.

A proposed reaction of thiosulfate with sodium carbonate is shown below:



#### CARBON DIOXIDE REDUCTION WITH CARBON

Carbon monoxide is an effective agent for the reduction of sodium sulfate to sulfide. To determine if carbon in a carbonate melt would reduce carbon dioxide to carbon monoxide, 6% carbon dioxide was added to the nitrogen purge stream. In a  $\text{Na}_2\text{CO}_3$  melt containing 4M, 3/8-inch carbon rods, but no sulfate, 2% of the carbon dioxide added was converted to carbon monoxide.

This experiment demonstrates that carbon in a carbonate melt will reduce carbon dioxide to carbon monoxide. Subsequently, carbon monoxide has been shown to be an effective reducing agent for sodium sulfate, forming sodium sulfide and carbon dioxide. Therefore, sulfate reduction can occur through a carbon monoxide-carbon dioxide cycle. Here, carbon monoxide reduces sulfate to form carbon dioxide, which is reduced by carbon to form additional carbon monoxide.

## MECHANISM OF SULFATE REDUCTION WITH CARBON

In this section a mechanism is proposed for sulfate reduction in the presence of carbon. This mechanism is based on the experimental results described in the previous section. A sulfate reduction model based on this mechanism is presented with the model parameters determined from the carbon dioxide and carbon monoxide evolution data. Finally, kinetic data from a series of experiments conducted to confirm the proposed sulfate reduction mechanism are presented.

### SUMMARY OF SULFATE REDUCTION

The basic characteristics of sulfate reduction with carbon are:

1) Sulfate: Depending on the sulfate concentration, sulfate reduction with respect to sulfate varies from first to zero order. At low sulfate concentration, reduction is first order in sulfate, whereas at high sulfate concentrations, reduction is zero order in sulfate.

This indicates that the sulfate reduction mechanism consists of at least two reactions in series, with only one of these reactions dependent on sulfate. At low sulfate concentrations, reduction is limited by the sulfate dependent reaction which is first order in sulfate. At high sulfate concentration, reduction is limited by the sulfate independent reaction.

2) Carbon Surface Area: Sulfate reduction was determined to be proportional to the square root of the carbon surface area.

3) Autocatalytic Nature of Sulfate Reduction: The most prominent characteristic of sulfate reduction with carbon is its autocatalytic behavior. Sulfate reduction begins with an induction period of about 6 minutes followed by a rapid



rate increase and a rate peak at about 30 minutes after the addition of the carbon. The rate then declines, reflecting the consumption of carbon and sulfate.

The autocatalytic nature results from the reaction of a reduction product or intermediate with sulfate or carbon, yielding a more reactive path for sulfate reduction. Since Birk et al. (4) reported that the autocatalytic nature of sodium sulfate reduction with hydrogen was due to sulfide, sulfide was considered the product most likely to account for the autocatalytic nature of sulfate reduction with carbon. However, the addition of various amounts of sulfide to the reaction system failed to produce any change in the characteristic reduction curve or reduction rate. Sulfide was found to behave as an inert in sodium sulfate reduction with carbon.

Another possibility examined was that the autocatalytic nature is due to a partially reduced sulfur compound. However, no partially reduced sulfur species such as sulfite were found in any melt sample. All the sulfur in the melt could be accounted for by sulfate and sulfide. When thiosulfate was added to the melt, it reacted with the carbonate to form sulfate and sulfide. Although some thiosulfate should be present in the melt when reduction was initiated by the introduction of carbon, the reduction rate curve for sulfate formed from thiosulfate has the same form as any sulfate reduction curve. Since no partially reduced sulfur compound was found in any melt sample and the addition of sulfide or thiosulfate failed to catalyze sulfate reduction, it is unlikely that a reduced sulfur compound is responsible for the autocatalytic nature of sulfate reduction with carbon.

In addition to sulfide, carbon dioxide and carbon monoxide are formed during sulfate reduction with carbon. In a previous study of sulfate reduction with carbon, Budnikoff and Shilov (6), it was found that carbon dioxide and carbon monoxide catalyzed sulfate reduction with carbon. Therefore, carbon monoxide and

carbon dioxide were considered likely candidates to account for the autocatalytic nature of sulfate reduction.

As shown in the experimental section, carbon monoxide will reduce sulfate, forming sulfide and carbon dioxide. Carbon will also reduce carbon dioxide, forming additional carbon monoxide. Therefore, sulfate reduction can occur by carbon monoxide reducing sulfate and forming carbon dioxide which is then reduced by carbon, forming additional carbon monoxide. In this mechanism, the autocatalytic behavior is due to an increase in carbon monoxide and carbon dioxide in the melt.

#### PROPOSED MECHANISM FOR SULFATE REDUCTION WITH CARBON

Based on the experimental results described in the previous section, the following mechanism is proposed for sodium sulfate reduction with carbon. The reduction reaction is initiated by the absorption of carbon dioxide in the melt onto the surface of the carbon. The absorbed carbon dioxide then reacts with the carbon to form two molecules of carbon monoxide. These carbon monoxide molecules then desorb from the carbon and react with sulfate in the melt to produce sulfide and additional carbon dioxide. The carbon dioxide and carbon monoxide are desorbed from the melt into the nitrogen purge stream.

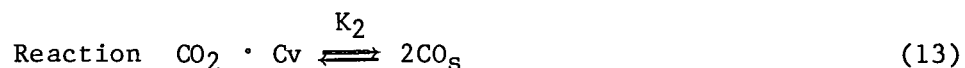
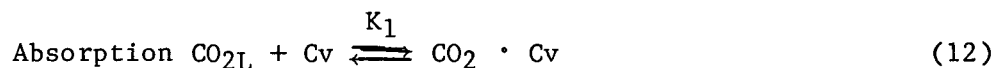
In this mechanism, the induction period is due to formation of sufficient quantities of carbon dioxide to initiate the reaction. This initial formation of carbon dioxide may result from the decomposition of the carbonate melt. At the temperatures employed in this study, all the carbonate melts produce a detectable level of carbon dioxide above the melt. Once reduction is initiated, a rapid rate increase occurs due to the increase in carbon dioxide and carbon monoxide in the melt. Since the concentrations of carbon dioxide and carbon monoxide in the melt

are greater than the concentrations which would be in equilibrium with the nitrogen purge stream, these gases are desorbed from the melt into the purge stream.

The proposed mechanism for sodium sulfate reduction with carbon can be divided into four stages: 1) the reaction between carbon dioxide and carbon, 2) sulfate reduction with carbon monoxide, 3) decomposition of sulfite and 4) desorption of carbon monoxide and carbon dioxide from the melt into the nitrogen purge stream. These four stages of sulfate reduction with carbon are described below.

#### Reaction of Carbon Dioxide with Carbon

Sulfate reduction begins with the absorption of carbon dioxide on a vacant reactive site on carbon. The absorbed carbon dioxide molecule reacts with the carbon to form two absorbed carbon monoxide molecules which desorb from the carbon into the melt. These steps are illustrated by Eq. (12) through (14).



where  $\text{CO}_{2\text{L}}$  is carbon dioxide dissolved in the melt,  
 $\text{Cv}$  is a vacant site on the carbon,  
 $\text{CO}_2 \cdot \text{Cv}$  is absorbed carbon dioxide on the carbon,  
 $\text{CO}_\text{s}$  is absorbed carbon monoxide on the carbon,  
 $\text{CO}_\text{L}$  is carbon monoxide dissolved in the melt.

In this type of mechanism one of the three reaction steps is normally considered to be the rate limiting step. To obtain a reduction rate dependent on the square root of the carbon surface area, desorption of carbon monoxide from the surface of carbon was chosen as the rate limiting step. Considering carbon monoxide

desorption to be an irreversible reaction, the carbon monoxide desorption rate is given by Eq. (15).

$$\text{Rate of carbon monoxide desorption} = K_3 [\text{CO}_s] \quad (15)$$

For Eq. (15) to be meaningful, the concentration of absorbed carbon monoxide  $[\text{CO}_s]$  must be written in terms of measurable quantities such as carbon dioxide in the melt  $[\text{CO}_{2L}]$  and total active sites on the carbon surface  $[\text{CT}]$ .

The total number of active sites on the carbon surface is equal to the sum of the vacant sites and the sites containing absorbed molecules, Eq. (16).

$$\text{CT} = \text{Cv} + \text{CO}_2 \cdot \text{Cv} + \text{CO}_s \quad (16)$$

Substituting for Cv and  $\text{CO}_2 \cdot \text{Cv}$  from Eq. (12) and (13), Eq. (16) becomes:

$$\text{CT} = \frac{[\text{CO}_s]^2}{K_2} + \frac{[\text{CO}_s]^2}{K_1 K_2 [\text{CO}_{2L}]} + [\text{CO}_s] \quad (17)$$

Solving Eq. (17) for absorbed carbon monoxide yields:

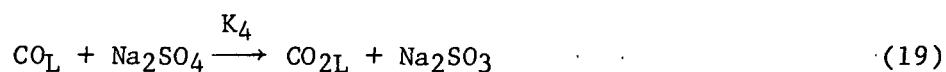
$$[\text{CO}_s] = \left[ -1 + \sqrt{1 + 4\text{CT} \left( \frac{K_1 [\text{CO}_{2L}] + 1}{K_1 K_2 [\text{CO}_{2L}]} \right)} \right] \frac{K_1 K_2 [\text{CO}_{2L}]}{2 (K_1 [\text{CO}_{2L}] + 1)} \quad (18)$$

Here, Eq. (18) predicts that the concentration of absorbed carbon monoxide will initially increase as the concentration of carbon dioxide in the melt increases.

However at high carbon dioxide concentrations, the absorbed carbon monoxide becomes independent of the carbon dioxide concentrations in the melt.

#### Sulfate Reduction with Carbon Monoxide

Once the carbon monoxide desorbs from the carbon, it reacts with sulfate in the melt, forming sulfite and additional carbon dioxide, Eq. (19).



In analyzing the experimental data in this study, this reaction was considered to be irreversible. The rate of sulfate reduction with carbon monoxide is given by Eq. (20).

$$\frac{d[\text{SO}_4]}{dt} = -K_4 [\text{CO}_L] [\text{SO}_4] \quad (20)$$

Here sulfate reduction is first order in terms of both carbon monoxide and sulfate.

#### Decomposition of Sulfite

Since sulfite is unstable above 150°C and no sulfite was found in any melt sample, it is assumed that little sulfite exists in the melt and that the rate of sulfite decomposition is faster than the rate of sulfate reduction.



Equation (21) is not a mechanism but represents a summary of rapid sequential events in sulfide decomposition.

#### Desorption of Carbon Monoxide and Carbon Dioxide from the Melt

As reduction proceeds, the concentration of carbon monoxide and carbon dioxide in the melt exceeds the concentration which would be in equilibrium with the purge stream or gas above the melt. The carbon dioxide and carbon monoxide in the melt are desorbed from the melt into the nitrogen purge stream. The rates of desorption for carbon monoxide and carbon dioxide are given by Eq. (22) and (23).

$$\frac{d[\text{CO}_{2g}]}{dt} = K_{\text{CO}_2} [\text{CO}_{2L} - \text{CO}_{2L}^*] A \quad (22)$$

$$\frac{d[\text{CO}_g]}{dt} = K_{\text{CO}} [\text{CO}_L - \text{CO}_L^*] A \quad (23)$$

where  $CO_{2g}$  is carbon dioxide in the gas phase,  
 $CO_g$  is carbon monoxide in the gas phase,  
 $CO_{2L}$  is carbon dioxide in the liquid phase,  
 $CO_L$  is carbon monoxide in the liquid phase,  
 $CO_{2L}^*$  is the concentration of carbon dioxide in the liquid phase which would be in equilibrium with the gas,  
 $CO_L^*$  is the concentration of carbon monoxide in the liquid phase which would be in equilibrium with the gas,  
 $K_{CO_2}$  is the mass transfer coefficient for carbon dioxide,  
 $K_{CO}$  is the mass transfer coefficient for carbon monoxide,  
 $A$  is the mass transfer area.

#### SULFATE REDUCTION MODEL

Based on the above mechanism, a model for sulfate reduction in a carbonate melt was developed. As illustrated in the proposed mechanism, sodium sulfate reduction with carbon involves transfer of reagents between three phases (solid, liquid, and gas) and a number of chemical reactions. It would be impossible to accurately define all the rate constants and mass transfer coefficients contained in this mechanism. Fortunately, many of these parameters are unnecessary to describe sulfate reduction in a sodium carbonate melt.

The model presented here describes reduction in terms of the evolution of carbon dioxide and carbon monoxide from the melt. This model describes reductions over the entire range of temperatures, sulfate concentrations, and carbon surface areas used in this study.

The model for sulfate reduction with carbon presented here consists of three stages: 1) the reaction between carbon dioxide and carbon, 2) sulfate reduction with carbon monoxide and 3) desorption of carbon dioxide and carbon monoxide

from the melt into the purge stream. The development of the reduction model from these stages is discussed below.

The amount of carbon monoxide absorbed on the carbon surface was given by Eq. (18). Since the reaction system was continuously swept with nitrogen, the carbon dioxide concentration in the melt remained low. Also excess carbon was used in these experiments, and the carbon surface area can be considered large. Therefore, under the experimental conditions of this study, the absorbed carbon monoxide represented by Eq. (15) can be approximated by Eq. (24).

$$[CO_s] = K' \sqrt{[C_T] [CO_{2L}]} \quad (24)$$

The rate of carbon monoxide desorption from the carbon surface is given by Eq. (25). At steady state in the carbon dioxide-carbon surface reaction, two molecules of carbon monoxide are desorbed for every molecule of carbon dioxide absorbed. The absorption rate of carbon dioxide, Eq. (26), is then equal to half the desorption rate of carbon monoxide.

$$\text{Carbon monoxide desorption rate} = K'' \sqrt{[C_T] [CO_{2L}]} \quad (25)$$

$$\text{Carbon dioxide absorption rate} = 1/2 K'' \sqrt{[C_T] [CO_{2L}]} \quad (26)$$

The rate equation for sulfate reduction in the model is the same as that proposed in the mechanism, Eq. (20). Sulfite decomposition is considered to be very fast and not to influence the sulfate reduction rate.

The driving force for desorption of carbon dioxide and carbon monoxide from the melt into the gas phase is the difference between the concentrations of these gases in the melt and the melt concentrations that would be in equilibrium with the partial pressures of these gases. From Henry's Law Eq. (27), it can be seen that

the equilibrium concentration of a dissolved gas is proportional to its partial pressure.

$$P_A = m X_A \quad (27)$$

Here:  $P_A$  is the partial pressure of Species A  
 $X_A$  is the mole fraction of A in the liquid  
 $m$  is Henry's Law constant

During the desorption of carbon dioxide and carbon monoxide from the melt, the concentrations of carbon dioxide and carbon monoxide in the purge stream remained low, normally less than 5%. Therefore, it was assumed that the equilibrium concentrations  $CO_{2L}^*$  and  $CO_L^*$  were low relative to the carbon dioxide and carbon monoxide concentrations in the melt.

Only small variations occurred in the nitrogen purge rate to the reactor. Also, experimental variations of 50% in the nitrogen purge had little effect on the sulfate reduction rate. Therefore, it was assumed that a large amount of the surface area for mass transfer was at the liquid-gas interface above the melt and the area was constant between reduction experiments. Under those conditions, the desorption of carbon dioxide and carbon monoxide from the melt can be represented by Eq. (28) and (29).

$$\frac{d[CO_{2g}]}{dt} = K[CO_{2L}] \quad (28)$$

$$\frac{d[COg]}{dt} = K'[CO_L] \quad (29)$$

Here,  $K$  and  $K'$  are mass transfer coefficients.



Using the conditions discussed above, sulfate reduction with carbon can be described by Eq. (30) and (31).

$$\frac{d[CO_L]}{dt} = K_1 \times \sqrt{[C_T] [CO_{2L}]} - K_2[CO_L] [SO_4] - K_3[CO_L] \quad (30)$$

$$\frac{d[CO_{2L}]}{dt} = -\frac{1}{2} K_1 \times \sqrt{[C_T] [CO_{2L}]} + K_2[CO_L] [SO_4] - K_4[CO_{2L}] \quad (31)$$

where  $K_1$  is the rate constant for monoxide desorption from the carbon surface,  
 $K_2$  is the rate constant for sulfate reduction with carbon monoxide,  
 $K_3$  is the mass transfer coefficient for carbon monoxide,  
 $K_4$  is the mass transfer coefficient for carbon dioxide.

Using an Arrhenius type temperature dependency for the rate constants  $K_1$  and  $K_2$ , the temperature effect was incorporated into the model. The mass transfer coefficients  $K_3$  and  $K_4$  were assumed to be relatively constant compared to the kinetic rate constants over the temperature range of this study. The sulfate reduction model including the Arrhenius activation energies is given by Eq. (32) and (33).

$$\frac{d[CO_L]}{dt} = K_1 \times e^{-\Delta E_1/RT} \sqrt{[C_T] [CO_{2L}]} - K_2 \times e^{-\Delta E_2/RT} [CO_L] [SO_4] - K_3[CO_L] \quad (32)$$

$$\frac{d[CO_{2L}]}{dt} = -\frac{1}{2} K_1 \times e^{-\Delta E_1/RT} \sqrt{[C_T] [CO_{2L}]} + K_2 \times e^{-\Delta E_2/RT} [CO_L] [SO_4] - K_4[CO_{2L}] \quad (33)$$

This model follows sulfate reduction through the variations in carbon dioxide and carbon monoxide in the melt. With this model, the evolution of carbon dioxide and carbon monoxide from the melt is given by Eq. (34) and (35).

$$\frac{d[CO_{2g}]}{dt} = K_4[CO_{2L}] \quad (34)$$

$$\frac{d[CO_g]}{dt} = K_3[CO_L] \quad (35)$$

Here, the mass transfer coefficients  $K_3$  and  $K_4$  are the same coefficients as in Eq. (32) and (33). The six parameters in Eq. (32) and (33) were determined by numerically integrating Eq. (32) and (33) and adjusting the parameters to minimize the difference between the predicted actual evolution of carbon dioxide and carbon monoxide from the reactor. The parameter optimization was accomplished using a nonlinear regression analysis program. The values of the parameters which best describe the kinetic data and their estimated linear standard derivations are given in Table V.

TABLE V  
PARAMETERS DESCRIBING SULFATE REDUCTION WITH CARBON

Parameter	Description	Estimated Value	Linear Estimate of Standard Deviation
$K_1$	Rate constant for carbon monoxide desorption from carbon	$0.036 \frac{(\text{g-mole})^{1/2} (\text{liter})^{1/2}}{\text{min}}$	0.0019
$K_2$	Rate constant for sulfate reduction with CO	$2.29 (\text{liter})^2/(\text{g-mole} \cdot \text{min})$	0.352
$K_3$	Mass transfer coefficient for desorption of CO from melt	0.019 (liter/min)	0.0045
$K_4$	Mass transfer coefficient for desorption of $\text{CO}_2$ from melt	0.46 (liter/min)	0.038
$\Delta E_1$	Activation energy for carbon monoxide desorption	40.0 kcal	3.5
$\Delta E_2$	Activation energy for carbon monoxide sulfate reaction	45.0 kcal	15.0

The sulfate concentration in the melt was calculated by subtracting 1/2 the sum of the carbon dioxide evolved and the estimated amount remaining in the melt and

$1/4$  the sum of the carbon monoxide evolved and the estimated amount remaining in the melt from the original sulfate concentration. The carbon surface area was also calculated based on the carbon dioxide and carbon monoxide evolved and the estimated amount remaining in the melt.

Actual and predicted levels of carbon dioxide and carbon monoxide evolution for typical reduction experiments are shown in Fig. 13-15. Although only three sets of data are shown, the sulfate reduction model and parameters in Table III accurately describe sulfate reduction over the entire range of temperature and concentrations used in this study.

#### EFFECT OF CARBON DIOXIDE ON SULFATE REDUCTION WITH CARBON

The basis of the proposed mechanism is that sulfate reduction occurs through a carbon dioxide-carbon monoxide cycle. This reaction is initiated by the absorption of carbon dioxide on the carbon surface. The absorbed carbon dioxide reacts with the carbon, producing two molecules of carbon monoxide. The carbon monoxide is desorbed from the carbon and reacts with sulfate, forming additional carbon dioxide. In this mechanism, the autocatalytic nature of sulfate reduction with carbon is due to the increase of carbon dioxide and carbon monoxide in the melt.

Two types of experiments were conducted to determine if the autocatalytic nature of sulfate reduction with carbon is due to the increase in carbon dioxide in the melt. In the first type of experiments different levels of carbon dioxide were added to the nitrogen purge stream. To ensure that carbon dioxide would be present in the melt prior to the introduction of carbon, the nitrogen purge containing the carbon dioxide was started ten minutes before the addition of the carbon. Once the carbon rods were added, the reaction was followed through the evolution of additional quantities of carbon dioxide and carbon monoxide.

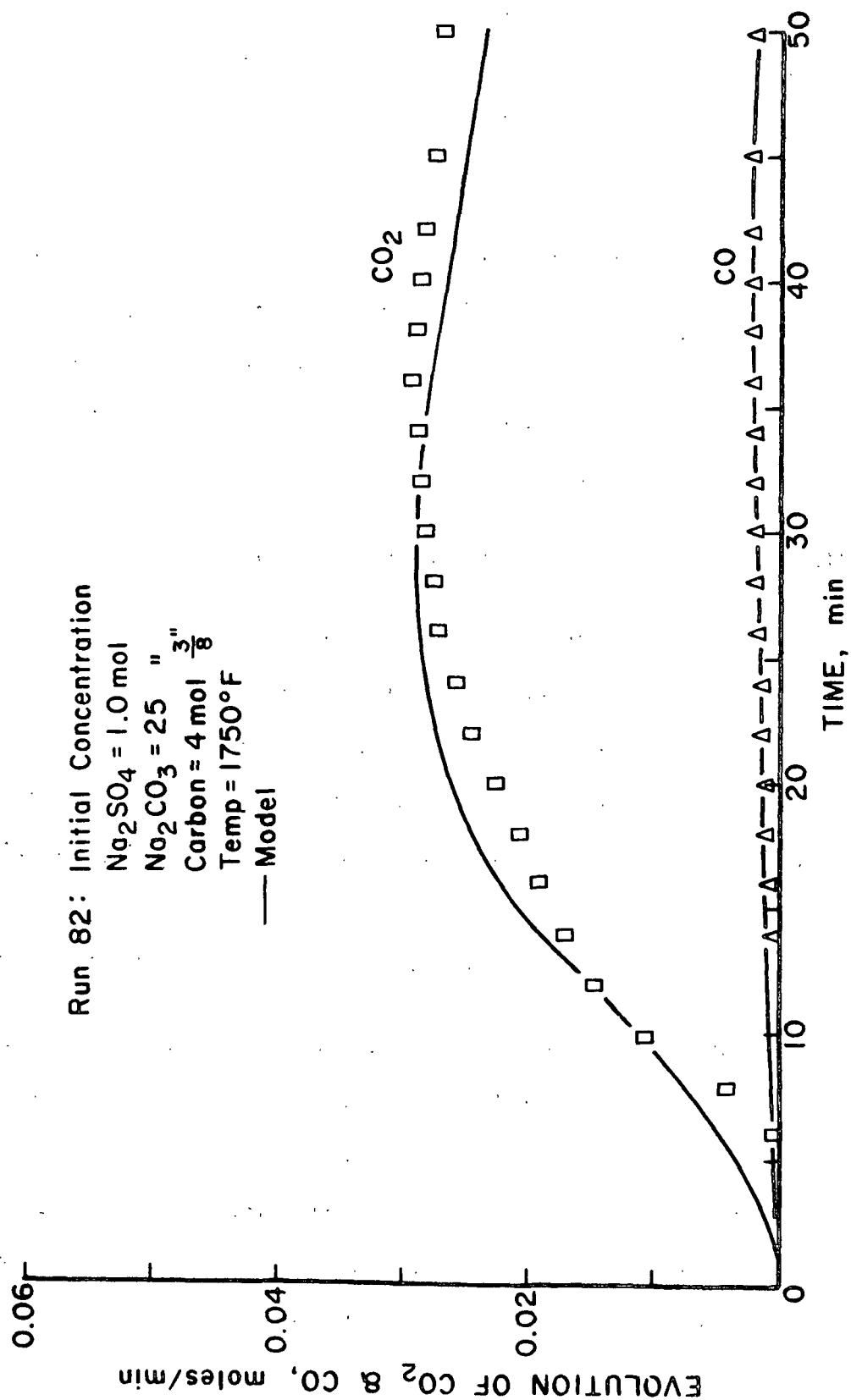


Figure 13. Sulfate Reduction with Carbon: CO<sub>2</sub> and CO Evolution vs. Time

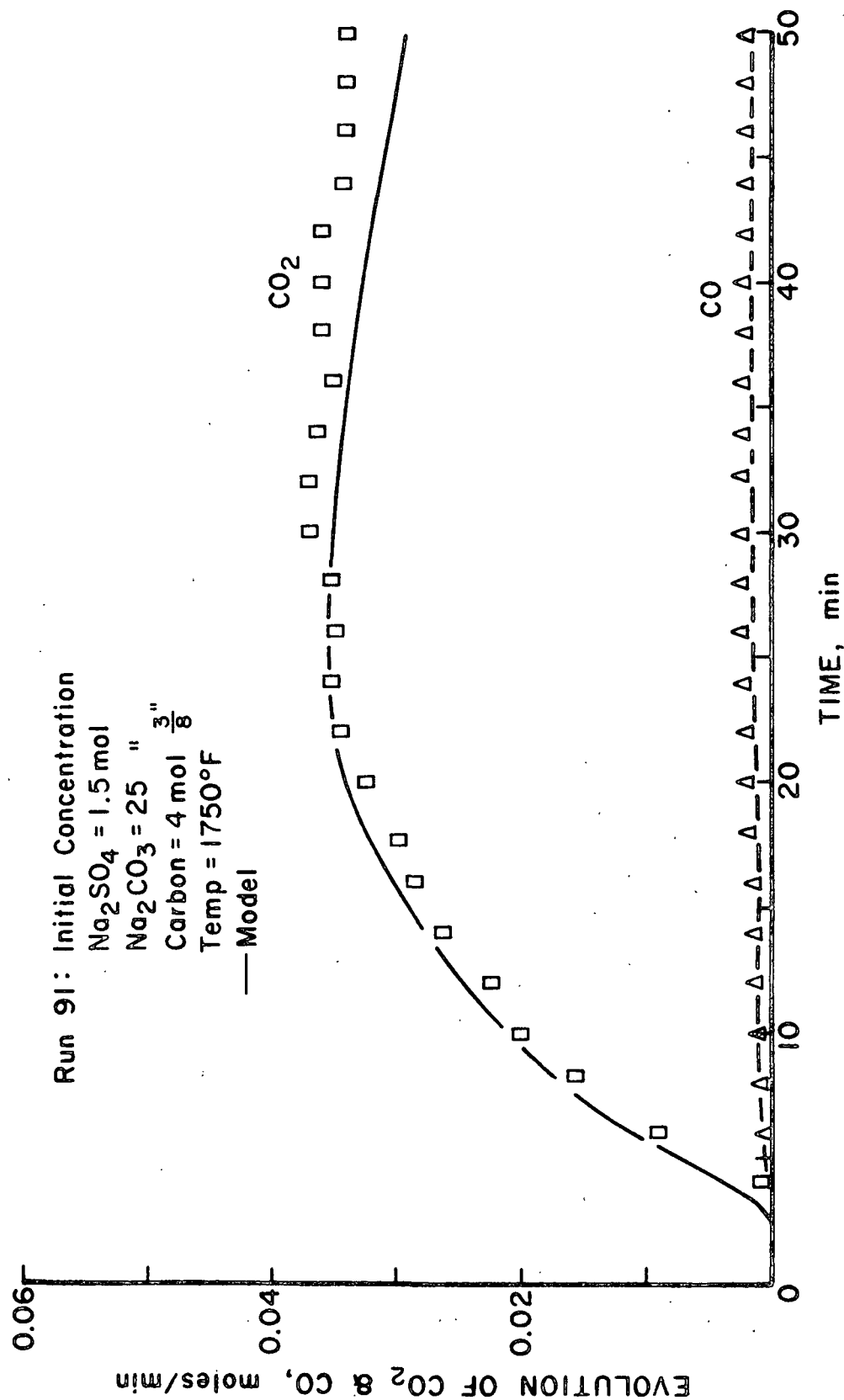


Figure 14. Sulfate Reduction with Carbon: CO<sub>2</sub> and CO Evolution vs. Time

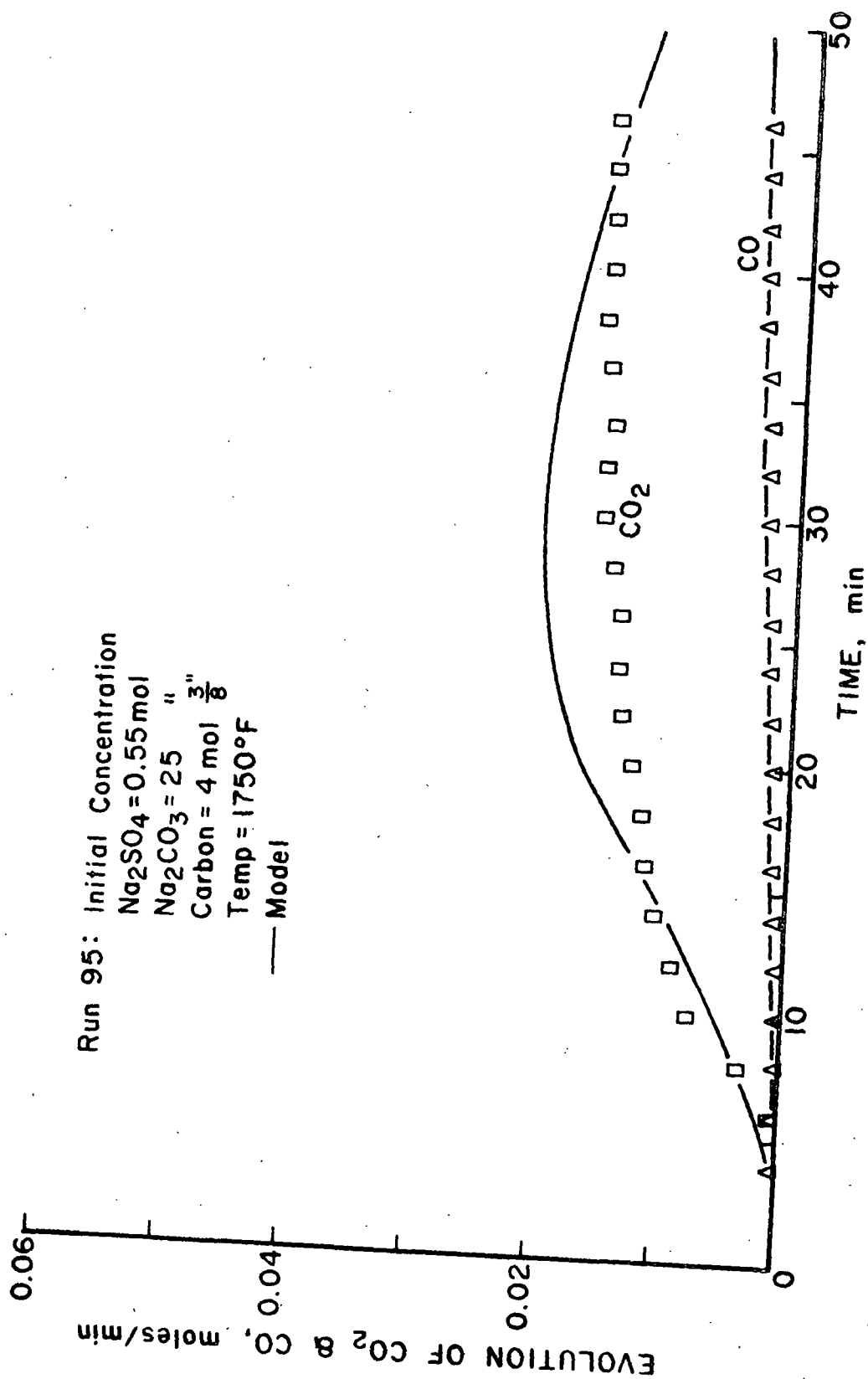


Figure 15. Sulfate Reduction with Carbon:  $\text{CO}_2$  and CO Evolution vs. Time

The effect of 5% and 10% molar addition of carbon dioxide to the nitrogen purge stream is shown in Fig. 16. The addition of carbon dioxide does initially increase the sulfate reduction rate, demonstrating that carbon dioxide will catalyze sulfate reduction with carbon.

After ten minutes, the sulfate reduction rate with carbon dioxide present in the purge stream is the same as that without carbon dioxide present. The maximum reduction rates with either 5% or 10% carbon dioxide added to the purge stream were 15% less than the maximum rate with no carbon dioxide added. This apparent decrease in the maximum reduction rate may be due to decrease in the gas desorption rate, Eq. (22), or to the reversibility of sulfate reduction with carbon monoxide, Eq. (29). The proposed mechanism for sulfate reduction predicts that at high levels of carbon dioxide, the amount of carbon monoxide absorbed on the carbon will remain constant as the level of carbon dioxide in the melt increases. Therefore at high levels of carbon dioxide, the sulfate reduction rate will no longer increase as the level of carbon dioxide in the melt increases. As the level of carbon dioxide in the purge stream increases, the carbon dioxide desorption rate from the melt decreases and sulfate reduction appears slower. If sulfate reduction with carbon monoxide, Eq. (29), is a reversible reaction, high levels of carbon dioxide will shift this reaction toward sulfate and carbon monoxide, resulting in a slower reduction rate.

At 5% or 10% addition of carbon dioxide to the purge stream, the decrease in reduction is slight. In this study, the level of carbon dioxide in the purge stream was normally 5% or less. Therefore, the apparent decrease in reduction rate at high levels of carbon dioxide was not incorporated into the proposed sulfate reduction model.

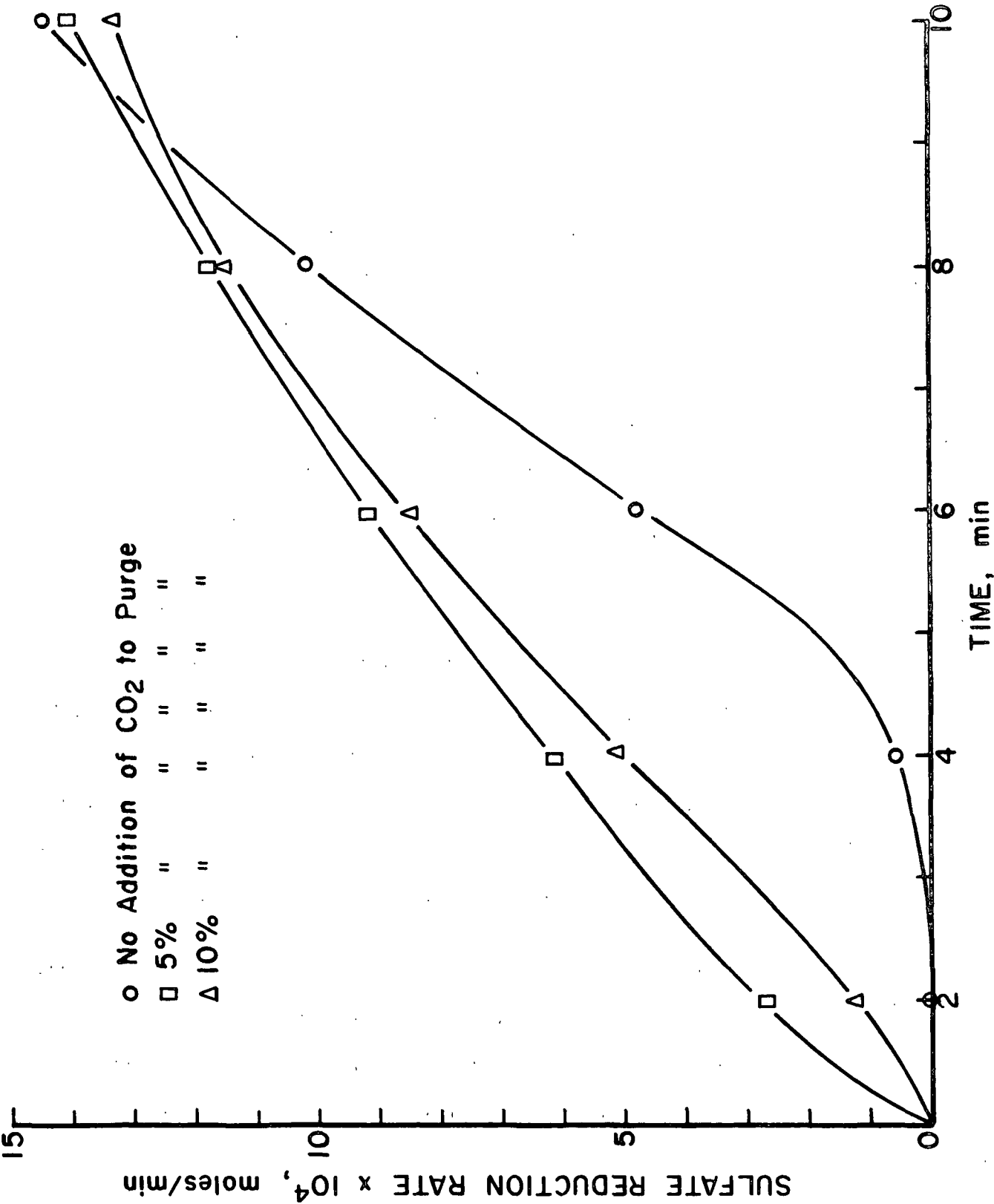


Figure 16. Effect of Carbon Dioxide Addition to Purge Stream



In the second type of experiment designed to demonstrate that the autocatalytic nature of sulfate reduction with carbon is due to an increase in carbon dioxide in the melt, an initial level of carbon dioxide was added to the melt before the introduction of the carbon rods. This carbon dioxide was added to the melt by purging the melt with pure carbon dioxide. To achieve the desired level of carbon dioxide in the melt, the carbon dioxide was then stripped from the melt with a nitrogen purge. Once the desired level of carbon dioxide was obtained, reduction was initiated by the introduction of the carbon rods.

The effect of this initial level of carbon dioxide is illustrated in Fig. 17. Here, the stripping of carbon dioxide is illustrated in Curve Ia, carbon dioxide evolution with an initial level of carbon dioxide present is illustrated in Curve Ib, and carbon dioxide evolution without an initial level of carbon dioxide is illustrated in Curve II. The effect of the initial level of carbon dioxide is evident in the comparison of the reduction rate with carbon dioxide initially present to the rate without carbon dioxide initially present. With carbon dioxide initially present reduction begins much faster. In Fig. 17 reduction without carbon dioxide initially present follows reduction with carbon dioxide initially present by about 8 minutes.

These experiments demonstrate that carbon dioxide will initially catalyze sulfate reduction with carbon. The autocatalytic nature of sulfate reduction with carbon is due to an increase in carbon dioxide and carbon monoxide in the melt. At high levels of carbon dioxide, the carbon surface becomes saturated with absorbed carbon dioxide and carbon monoxide, and the reduction rate no longer increases as the level of carbon dioxide in the melt increases.

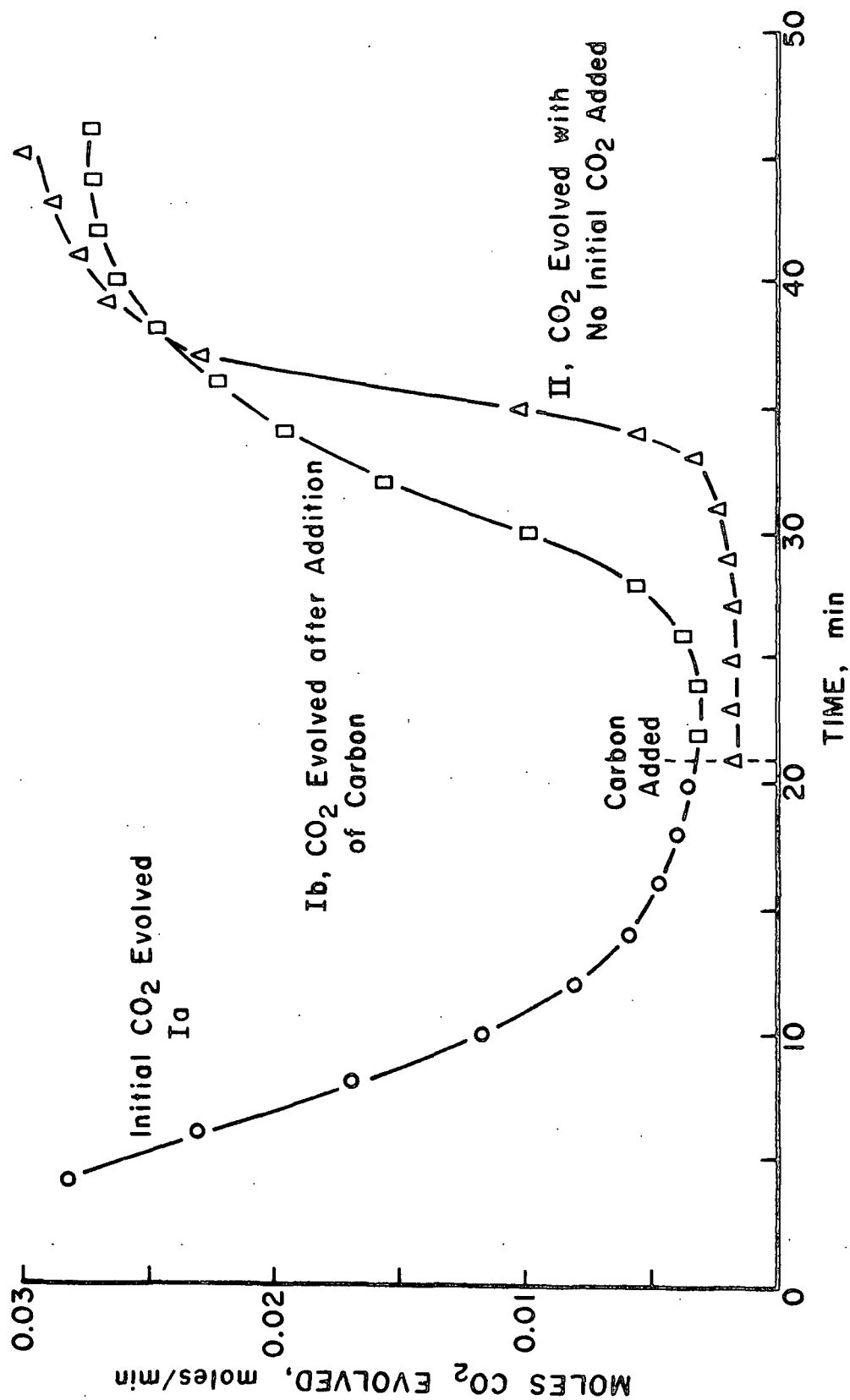


Figure 17. Effect of Carbon Dioxide on Sulfate Reduction Rate

#### APPLICATION TO RECOVERY FURNACE

The intent of this section is to show how the information gained from this study of sulfate reduction kinetics and mechanism can be applied to the conditions which exist within the recovery furnace. Not only will this suggest furnace parameters which will maximize the reduction efficiency, but it will also provide insight on rates of char burnup, char bed stability and blackout prevention.

#### CRITICAL KINETIC PARAMETERS

The kinetic rate expressions developed in the course of this work and their mechanistic interpretation make it possible to proceed with confidence to apply the results of the laboratory study to the char bed. In particular, a simplified kinetic expression can be developed for char bed conditions. The simplification is based on the following facts and assumptions.

1. The reduction of sulfate by carbon is endothermic with a heat of reaction of about 520 Btu/lb  $\text{Na}_2\text{SO}_4$  for  $\text{CO}_2$  as the reaction product, and 1540 Btu/lb  $\text{Na}_2\text{SO}_4$  for CO as the product.
2. The temperature sensitivity of the reaction rates can be expressed in terms of an Arrhenius type activation energy with a magnitude of about 50 kcal/mole.
3. The rate equation becomes first order in sulfate concentration as the sulfate becomes depleted. Since relatively high reduction efficiencies are attained in the recovery furnace, sulfate concentrations will become small.

4. The rate is dependent on the square root of the carbon surface area. In the char bed there should be an excess of carbon present, and the reaction should not be limited by carbon depletion. Accordingly, the effect of changing carbon content can be neglected in a simplified rate equation.
5. It is assumed that the pyrolysis process supplies sufficient CO and CO<sub>2</sub> to the smelt so that the induction period in the reaction kinetics is eliminated.

Under these conditions, the kinetic equation for the reduction of sulfate by carbon can be simplified to:

$$\frac{-d[\text{Na}_2\text{SO}_4]}{dt} = K_1 e^{-\Delta E/RT} [\text{Na}_2\text{SO}_4] \quad (36)$$

where  $[\text{Na}_2\text{SO}_4]$  = sulfate concentration, mole/mole smelt,

$K_1$  = constant,

$\Delta E$  = activation energy,

$R$  = gas constant,

$T$  = absolute temperature.

It will be shown that under many conditions, the thermal effects completely dominate the kinetics. Under these conditions, the two parameters that control the reaction kinetics are the activation energy,  $\Delta E$ , and the heat of reaction,  $\Delta H_R$ . (The latter is dependent on the CO<sub>2</sub>/CO ratio in the product gas.)

#### Activation Energy

For all practical purposes the activation energy can be taken to the 50 kcal/mole which gives the reaction rate doubling for about a 70°F rise (at 1700°F).

The rate would drop by about an order of magnitude for a 200°F drop from 1700 to 1500°F.

### Heat of Reaction

The heat of reduction for sulfate can be expressed in terms of the percent of CO in the product gas as follows:

$$\Delta H_R, \frac{\text{Btu}}{\text{lb Na}_2\text{SO}_4} = 1550 - 2050 \frac{(100 - \% \text{CO})}{(200 - \% \text{CO})} \quad (37)$$

This expression is obtained by combining the heats of reaction for the first two reactions in Table II (page 10). The very minor effect of temperature on the heat of reaction is ignored. There is little information available on the proportions of CO and CO<sub>2</sub> in the char bed of a recovery furnace. In one very limited experiment which we did, about equal amounts of CO and CO<sub>2</sub> were found. This would give a heat of reaction of 867 Btu/lb Na<sub>2</sub>SO<sub>4</sub>.

### HEAT TRANSFER EFFECTS

The impact of thermal effects on the overall rate of reaction can best be seen by considering an isolated system in which no heat enters or leaves. In this case the heat balance becomes:

$$\Delta H_R \frac{d}{dt} [\text{Na}_2\text{SO}_4] = M C_p \frac{dT}{dt} \quad (38)$$

where  $M$  = mass of reaction system,

$C_p$  = specific heat of the system.

The concentration of sulfate at any time,  $t$ , can be found by integrating Eq. (38).

$$\int_0^t \frac{d}{dt} [\text{Na}_2\text{SO}_4] dt = \frac{M C_p}{\Delta H_R} \int_0^t \frac{dT}{dt} dt \quad (39)$$

or

$$[\text{Na}_2\text{SO}_4] - [\text{Na}_2\text{SO}_4]_0 = \frac{M C_p}{\Delta H_R} (T - T_0) \quad (40)$$

Thus, in an isolated system there is a one-to-one correspondence between sulfate concentration and temperature which depends only on the initial temperature, the initial sulfate concentration, and the parameter  $M C_p / \Delta H_R$ .

Noting that the final temperature,  $T_F$ , is given by the solution to Eq. (40) when  $[\text{Na}_2\text{SO}_4]$  is zero, it is seen that:

$$(T_0 - T_F) = \frac{\Delta H_R [\text{Na}_2\text{SO}_4]_0}{M C_p} \quad (41)$$

The significance of  $(T_0 - T_F)$  is that it is the total temperature drop that would occur if all of the sulfate in the system were reduced adiabatically. Then Eq. (40) can be rewritten as:

$$\frac{[\text{Na}_2\text{SO}_4]}{[\text{Na}_2\text{SO}_4]_0} = \frac{(T - T_F)}{(T_0 - T_F)} \quad (42)$$

Putting Eq. (38) and (42) into the original kinetic expression [Eq. (36)], one obtains:

$$\frac{dT}{dt} = -K_1 (T - T_F) e^{-\Delta E/RT} \quad (43)$$

This expression shows how the behavior of temperature (and since temperature and sulfate are in one-to-one correspondence, the sulfate concentration, too) changes with time for an adiabatic reaction.

If the activation energy were negligible, the temperature would decay exponentially to  $T_F$  from  $T_0$ , i.e.,

$$\frac{(T - T_F)}{(T_0 - T_F)} = e^{-K_1 t} \quad \text{when } \Delta E = 0 \quad (44)$$

When  $\Delta E$  is not zero, the final approach to  $T_F$  will be much slower. The greater the value of  $\Delta E$ , the greater the degree of kinetic control.

It is of interest to look at how the rate at time  $t$  compares with the initial rate.

$$\frac{(dT/dt)}{(dT/dt)_0} = \frac{(T - T_F)}{(T_0 - T_F)} e^{\frac{-\Delta E [T_0 - T]}{R T_0 T}} \quad (45)$$

The contribution of the activation energy term to the declining rate for two different initial temperatures is shown below for  $\Delta E = 50,000$  cal/mole.

$(T_0 - T), ^\circ F$	$e^{\frac{-\Delta E [T_0 - T]}{R T_0 T}}$	
	$T_0 = 1800^\circ F$	$T_0 = 2000^\circ F$
100	0.395	0.458
200	0.1426	0.196
300	0.0465	0.0774
400	0.0134	0.0279
500	0.0033	0.0091

The temperature drops in the above tabulation may be compared with some estimates of the adiabatic temperature drop for complete reduction  $(T_0 - T_F)$ . Two cases are considered.

Case 1: sulfidity (on TTA) = 30%, no sulfide, all sulfate,  
carbon content 15% by weight,  
then  $[Na_2SO_4] = 0.31$  lb/lb bed  
and  $(T_0 - T_F) = \frac{0.31 \times \Delta H_R}{1 \times 0.3} = 1.033 \Delta H_R$   
three values for  $\Delta H_R$  may be used to bracket the  
effect: 525 Btu/lb for all  $CO_2$ , 1550 Btu/lb for all  
 $CO$  and 867 Btu/lb for 50-50  $CO_2$  and  $CO$ . This gives  
 $(T_0 - T_F) = 543, 1602$  and  $896^\circ F$ , respectively.

Case 2: sulfidity (on TTA) = 30%, 50%  $Na_2S$  and 50%  $Na_2SO_4$   
carbon content 10% by weight,  
then  $[Na_2SO_4] = 0.179$  lb/lb bed  
and  $(T_0 - T_F) = 0.179$  lb/lb bed,

$$(T_o - T_F) = \frac{0.79 \times \Delta H_R}{1 \times 0.3} = 0.5967 \Delta H_R$$

$$(T_o - T_F) = 313, 925 \text{ and } 517^\circ\text{F, respectively.}$$

The importance of accurate knowledge of the heat of reduction under the conditions that it occurs in the furnace is clearly evident in the above calculations. The uncertainty that exists with regard to the heat of reduction makes it impossible to accurately interpret temperature drop data.

The calculations done above also show that the activation energy term will tend to dominate thermal effects. It is also evident that it is advantageous to start at a higher initial temperature. Not only will the initial rate be higher, but the rate will drop less sharply for the same temperature change.

The analysis presented above is for the adiabatic case and shows that the temperature drop associated with the endothermic heat of reduction will cause the reaction rate to decline by as much as two orders of magnitude. Unless the initial temperature is high enough that the reduction rate is extremely rapid, the declining reaction rate with temperature will essentially become self-limiting in any reasonable time. However, if heat can be transferred into the reaction mass at reasonable rates, the reaction endotherm can be supplied without as great (or any) temperature drop, and the reaction will proceed at reasonable rates.

Thus, one can distinguish two different ways that reduction can occur in a recovery furnace.

1. The initial temperature of the smelt-char reacting mass is high enough that reduction can proceed rapidly toward completion even



though the temperature drops significantly as the reaction proceeds.

2. The temperatures at which the reaction occurs are moderate, and reduction will approach completion only if external heat is supplied. In the limit, the rate of the reduction reaction will be completely controlled by the rate of heat transfer.

It is necessary to examine data from operating char beds to sort out these effects.

#### CHAR BED DATA

Relatively little information on char beds exists. Borg et al. (9) reported on the results of Swedish work in 1974. More recently A. D. Little has carried out a study of recovery processes for the API Recovery Boiler Committee that has involved some measurements on char beds. The Institute of Paper Chemistry assisted in this work.

No actual data on char bed composition were given in the Swedish paper. They state, however:

"A number of samples of the bed and smelt have been analyzed. The composition of the smelt is fairly constant. Smelt reduction is lower and more variable than that of the bed. Besides the major components,  $\text{Na}_2\text{CO}_3$  and  $\text{Na}_2\text{S}$ , both smelt and bed contain a few percent  $\text{Na}_2\text{SO}_4$  and  $\text{NaOH}$ , but no other sodium compounds. The carbon (char) content of the bed was found to be around 5% by weight, except at unusually low bed temperatures, e.g., in local 'cold spots' where the percentage is higher, about 8%. The bed

may be described as a very porous char-bed where the carbon (char), to a certain extent, forms a 'lattice'."

They do provide one set of data on the composition of the gas phase just above the bed.

COMPOSITION OF GAS PHASE ABOVE THE BED

	Observed
H <sub>2</sub> , %	3
H <sub>2</sub> O, %	4
CO, %	6
CO <sub>2</sub> , %	13
O <sub>2</sub> , %	5
N <sub>2</sub> , %	68
CH <sub>4</sub> , %	0.1
H <sub>2</sub> S, ppm	300
SO <sub>2</sub> , ppm	1
Na and NaOH, % of Na to furnace	1.5

The data of A. D. Little is somewhat more extensive. The initial study was concerned with char bed cooling after a shutdown and included measurements of bed thermal properties and some temperature profiles. They concluded that the char beds in B&W recovery boilers generally were significantly different in character from those in CE units.

Char beds in B&W units were generally considerably larger and contained an inactive core which was at a temperature below 1400°F, i.e., lower than the usual

melting point and the temperature at which smelt ran out of the furnace. The inactive core had a low thermal conductivity of about 0.05 Btu/hour feet °F, a fairly high density of about 50-80 lb/ft<sup>3</sup> and thus a low porosity, 30-40%.

Char beds in CE recovery boilers were generally considerably smaller and hotter and normally did not contain an inactive core. The apparent thermal conductivity was 0.16-0.22 Btu/hour feet °F, the density was much lower, as low as 20 lb/ft<sup>3</sup>, and the porosity was very high, 75-85%.

They found that the thermal conductivity of the char was inherently low, but that there could be a substantial contribution to heat transfer within the bed due to radiation. The radiation component increased rapidly with temperature and also increased with porosity. The effect of the internal radiation was to make the apparent thermal conductivity of the bed material increase rapidly with temperature, especially in beds with a high void fraction (high porosity). This behavior could be summarized by the following equation.

$$k = 0.05 + 4 \Phi D_p \sigma T^3 \quad (46)$$

where  $\Phi$  = porosity or void fraction,

$D_p$  = pore size,

$\sigma$  = Stefan-Boltzmann constant,

$T$  = absolute temperature,

$k$  = thermal conductivity.

Without the contribution from radiation, the thermal conductivity is equivalent to that of high temperature insulating material.

A series of bed temperature profiles were obtained in a B&W unit at Weyerhaeuser's Longview, Washington, Mill. This is a B&W, "low-odor" unit operating

with a relatively low bed and with a minimum of wall drying. The profiles are shown in Fig. 18. There is a good deal of variability because the beds are not that homogeneous. In addition, the distances given are distances that the probe was inserted into the furnace, and the exact location of the probe tip is impossible to determine. In some cases it obviously came back out of the bed.

In general, the profiles rapidly reach a peak between 1800 and 2000°F and then fall off, approaching gradually the smelt discharge temperature. The distance over which the temperature drop occurs varies from about 1 to 3 feet.

Data on the composition of samples from in and around the bed are shown in Table VI. "Fines" is a term A. D. Little used to describe the material falling on the bed. Smelt samples were taken at the spout.

A number of features are evident in these data.

1. There is relatively little carbon in the bed. With one exception, the carbon content of the bed is less than 10% by weight, and most values are close to 5%. This is in general agreement with the findings of Borg, Teder, and Warnquist.
2. The state of reduction of the bed material is high. At Longview, except for Sample 10, all of the bed samples show large amounts of sulfide and relatively little sulfate. The data at Luke are more equivocal.
3. The carbon content and state of sulfur oxidation of the material coming to the bed are substantially higher than in the bed itself. Thus, a considerable amount of the

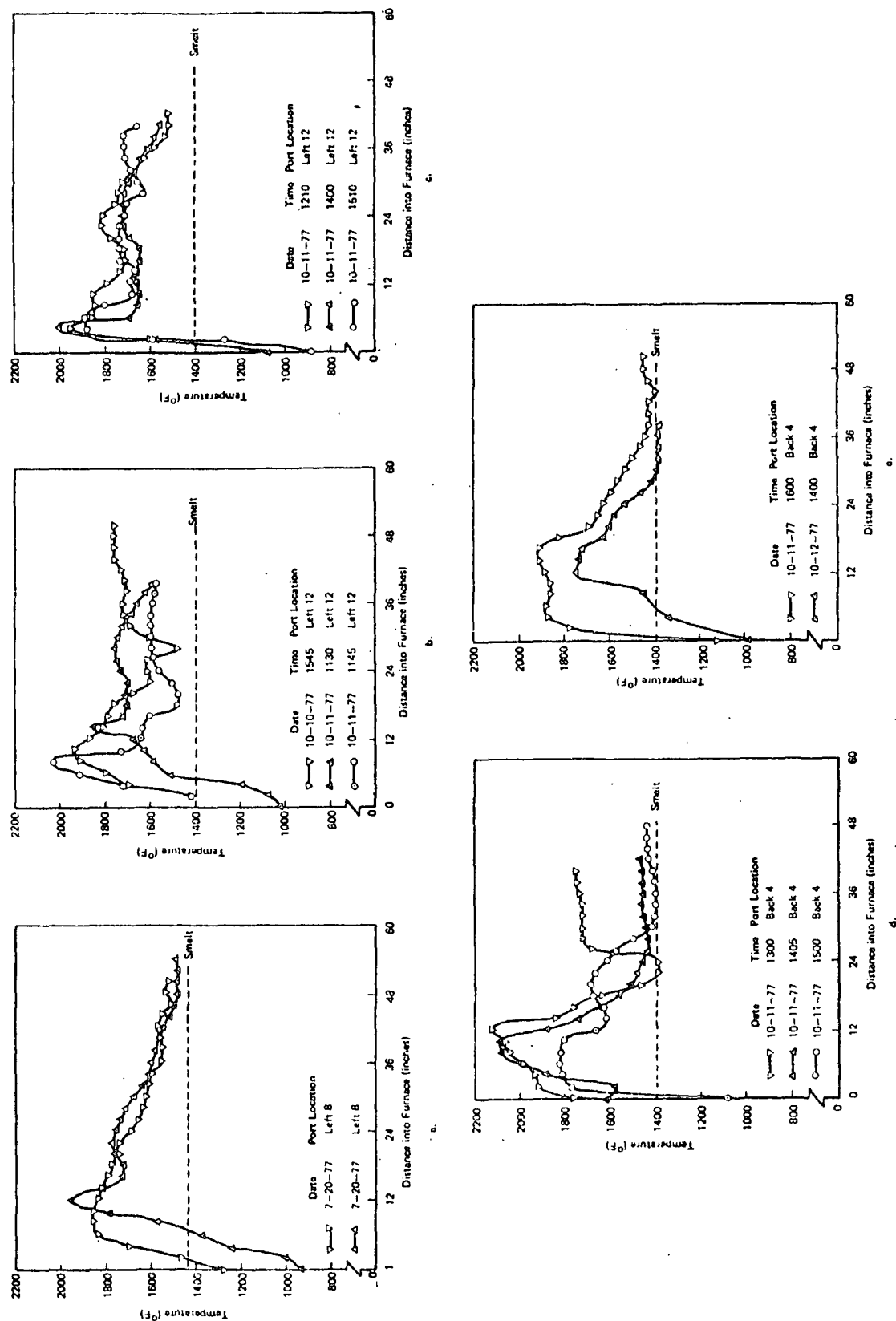


Figure 18. Measured Bed Temperatures - Weyerhaeuser Furnace

TABLE VI

SUMMARY OF SAMPLE ANALYSES FROM MILL VISITS (WEIGHT PERCENT)

Sample Number	Location	Na <sub>2</sub> CO <sub>3</sub>	Na <sub>2</sub> S	Na <sub>2</sub> SO <sub>4</sub>	Na <sub>2</sub> S <sub>2</sub> O <sub>3</sub>	Na <sub>2</sub> SO <sub>3</sub>	NaOH	Carbon
Weyerhaeuser, Longview (10-12-77)								
1	Bed sample - rear port No. 4, 36 inches into boiler	66.1	17.7	0.81	2.4	0.3	--	5.06
2	Bed surface sample - rear port No. 4	70.9	16.4	2.11	2.1	0.2	--	6.72
3	Fines - first secondary port, left side (front)	70.3	3.9	8.55	6.7	1.0	--	11.1
4	Bed sample - left side port No. 12, 36 inches into boiler	41.8	18.3	0.30	2.4	0.2	--	5.7
5	Bed sample - left side port No. 12, 18 inches into boiler	57.6	20.1	0.20	1.5	0.2	--	4.38
6	Bed sample - rear port No. 4, 32 inches into boiler	54.8	15.3	1.11	3.2	0.7	--	8.29
7	Bed surface sample - left side port No. 12	57.7	16.8	1.26	2.4	0.3	--	9.43
8	Fines - secondary air port, left side near rear	51.9	14.2	6.59	2.6	0.5	--	5.56
9	Smelt sample	63.4	20.3	2.94	0.2	0.2	--	--
10	Bed sample - front primary No. 3, near right-hand side	55.7	12.0	6.52	2.1	0.3	--	12.6
11	Fines/chunk - secondary air No. 1, front near right-hand side	58.8	4.9	6.02	7.3	0.3	--	15.5
14	Black liquor	--	3.6	2.2	2.7	<0.2	--	--
Westvaco, Luke, MD (6-30-78)								
-	Smelt	79.1	14.8	2.22	trace	trace	--	0.60
1	Fines	81.4	6.80	3.92	1.71	0.22	--	5.96
2	Bed	83.6	7.68	0.71	3.46	0.06	--	4.50
4	In bed	81.3	5.83	2.65	2.96	0.17	--	7.07
5	Fines	80.0	0.99	7.29	3.52	trace	--	8.24
7	Bed surface	80.3	5.42	1.18	4.93	0.30	--	7.86
Probe	Probe at end of 82 hours	76.1	3.73	2.52	4.23	trace	--	13.38

reduction and the carbon burnup is taking place in the char bed.

#### ADL Model

A. D. Little has developed a mathematical model of the processes occurring in the char bed of a recovery furnace. The model predicts that the bed has a finite capacity for reduction, and that the factors which are most important in determining the overall reduction efficiency are the sulfur to sodium ratio and the state of reduction of the material arriving on the bed. The model indicates that there is relatively little heat transfer into the bed by conduction or by combustion occurring within the bed.

The model prediction of a finite capacity for reduction in the bed is a consequence of some assumptions that effectively thermostat the bed surface temperature and which result in CO being the product of the reduction reaction and hence assume the largest possible endotherm. However, the model results clearly show that the extent of reduction within the bed is almost totally controlled by thermal parameters and heat transfer effects.

All of the data on char beds are consistent with the following.

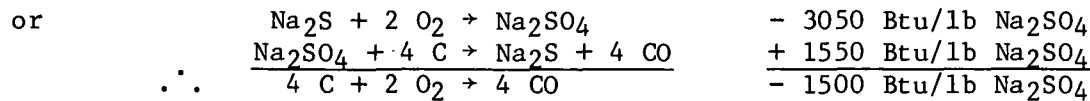
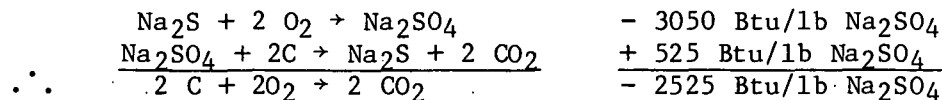
1. Reduction occurs as a net endothermic reaction in the char bed. The active zone is confined to the outer 1-2-foot-thick region of the bed.
2. Reduction occurs more rapidly (and thus creates a heat sink) than heat can flow into or be generated within the bed. As a consequence, bed temperature decreases from the surface inward. The interior of a char bed is cooler than the surface.

3. The main parameters influencing the rate and extent of reduction in the char bed are the bed surface temperature and the porosity of the char bed. The surface temperature determines the initial rate and the magnitude of the temperature drop before slow kinetic rates are obtained. The combination of higher temperatures and high porosity aids heat flow into the bed.
4. The degree of reduction in the interior of the char bed may be higher than it is in the smelt leaving the unit. This suggests some sulfide reoxidation is taking place.

#### CHAR COMBUSTION

In the char bed, the reduction of sulfate to sulfide occurs simultaneously with the oxidation of carbon to carbon monoxide and carbon dioxide. The sulfate can be looked upon as the oxygen supply for gasifying and burning the carbon. In fact, reaction with sulfate is the main route by which carbon is oxidized in the furnace.

This process can occur cyclically, with sulfate-sulfide interchange serving as an oxygen carrier from combustion air to the carbonaceous char. The oxidation of sulfide to sulfate is exothermic while the reduction of sulfate to sulfide is endothermic. The net result in a cyclic process is exothermic as can be seen from the following reactions.





Thus, the sulfate-sulfide cycle can serve as a catalyst for the burning of carbon in the bed. The net result is exothermic (i.e., heat liberating). This cyclic process can go on with most of the sulfur as sulfide (high reduction efficiency) and with the atmosphere oxidizing enough that 90-95% of the carbon is burned to  $\text{CO}_2$ . This has been demonstrated experimentally in work at Atomics International.

What this means is that a substantial amount of net reduction could take place on the upper layer of the char bed (perhaps a few inches deep) at relatively high temperatures where combustion air strikes the bed and burns char. Combustion processes can supply a substantial part of the heat required for reduction within the bed as well, if air is able to penetrate the bed.

Another consequence of sulfate being the main oxygen source for char combustion is that the kinetics of char combustion will be virtually the same as the kinetics for sulfate reduction. In particular, the activation energy and hence the temperature dependence of the char combustion rate will be the same as that for reduction. The lower temperature limit at which the reaction rate becomes vanishingly small (about 1450-1500°F) would be the same in both cases. This might well be related to the blackout phenomenon. If the bed surface temperature in a particular area of the bed drops into the 1450-1550°F region, char combustion would stop and the dark area could spread.

It should be noted that carbonaceous char is not the only combustible component of the char bed. The  $\text{Na}_2\text{S}$  present is also combustible with an exothermic heat of reaction of 5550 Btu/lb  $\text{Na}_2\text{S}$  oxidized. Our data suggest that sulfide reoxidation is inherently a fast reaction and proceeds at a rate controlled by mass transfer of oxygen to the sulfide. Local sulfide reoxidation is strongly exothermic

and can result in a hot spot developing. As the following calculation indicates, the oxidation of sulfide corresponding to a drop of 5% in reduction efficiency can raise smelt temperature by as much as 200°F.

Basis: 1 lb smelt, at 30% sulfidity, and with initial reduction efficiency of 100%.

$$\text{Na}_2\text{S present: } 1 + \frac{106}{78} \frac{(1 - 0.7)}{0.3} = 0.24 \frac{\text{lb Na}_2\text{S}}{\text{lb smelt}}$$

$$5\% \text{ drop in reduction efficiency} = 0.05 \times 0.24 = 0.012 \text{ lb Na}_2\text{S oxid.}$$

$$0.012 \times 5550 \frac{\text{Btu}}{\text{lb Na}_2\text{S}} = 1 \text{ lb} \times 0.32 \frac{\text{Btu}}{\text{lb } ^\circ\text{F}} \times \Delta T$$

$$\therefore \Delta T = 208^\circ\text{F}$$

The fact that a small amount of reoxidation can result in a large temperature increase complicates the interpretation of furnace temperature data. High temperatures are beneficial for reduction so long as carbon is present and reduction can be maintained. When carbon is absent, high temperatures may simply reflect the fact that reduction efficiency was lost due to reoxidation.

#### OVERALL REDUCTION EFFICIENCY

All of the available information indicates that the extent of sulfate reduction in the char bed of a kraft recovery boiler is controlled by energy transfer into the bed. The single most important parameter for good reduction is bed surface temperature. High surface temperatures not only give the highest initial reaction rates but also give more sensible heat to draw on before the temperature drops to values where the kinetics become very slow. In addition high temperature levels increase the rate of heat transfer into the bed by increasing the apparent bed thermal conductivity due to internal radiation.

There is reason to believe that low bulk density, high porosity beds are beneficial. High porosity increases the apparent bed thermal conductivity, especially at higher temperatures. It also increases the likelihood of air penetrating the bed and generating heat by combustion.

There is no evidence to indicate that a large char bed is needed to achieve high reduction efficiencies. The region of the char bed that is chemically active is the outer foot or two in thickness. The remainder is effectively inert. The interior of a large char bed (especially in a B&W unit) is normally below the smelt melting temperature. It acts as a "deadman," taking up space and providing inventory. It does not take part in the process reactions. The only beneficial role that a large bed might play is by serving as a shield to help prevent reoxidation.

The net reduction efficiency obtained from a recovery furnace depends on the extent of reoxidation as the smelt flows out of the bed and out of the furnace. Relatively large quantities of air are introduced at the primary level and can contact molten smelt and reoxidize it. The shielding action of a large bed may help reduce this somewhat.

Reoxidation will tend to increase smelt temperature. This can obscure the beneficial effect of bed temperature on reduction. Smelt temperatures could increase due to reoxidation (giving a lower reduction efficiency) or because of higher bed temperatures (giving a higher reduction efficiency). Thus there may be no general correlation between smelt temperature and reduction efficiency.

### CONCLUSIONS

1. Sulfate reduction with carbon occurs through a carbon dioxide-carbon monoxide cycle. This cycle is initiated by the absorption of carbon dioxide on the surface of carbon. This absorbed carbon dioxide reacts with the carbon to form two molecules of adsorbed carbon monoxide. The carbon monoxide desorbs from the carbon and reacts with sulfate in the melt to form sulfite and carbon dioxide. This sulfite undergoes a fast decomposition reaction to form sulfide and sulfate. The autocatalytic nature of sulfate reduction with carbon is due to the increase in carbon dioxide and carbon monoxide in the melt.
2. The reduction of sulfate in the char bed of a recovery furnace is governed by thermal effects. The combination of an endothermic reaction and strongly temperature sensitive kinetics (high activation energy) causes the reaction to become self-limiting unless heat is added. The extent of reaction is determined by the initial amount of sensible heat available in the reacting mass and the rate of heat transfer into the material.
3. The most important single parameter influencing reduction in the kraft furnace is the bed surface temperature. This sets the initial rate of reaction, determines the amount of sensible heat available for the endothermic reaction to draw on, and influences the apparent thermal conductivity of the bed. High bed surface temperatures are favorable to reduction.
4. There is a good deal of uncertainty as to the magnitude of the endothermic heat of reaction in the char bed. This is because the heat of reaction is strongly dependent upon the relative amounts of CO and CO<sub>2</sub> produced. There is a need for experimental data on this point.

5. There is no need to have a large char bed in order to have a high reduction efficiency. The portion of the bed that is chemically active is only a foot or so thick. The remainder is inactive and serves merely to occupy space, provide inventory, and require considerably longer cool down (or burn down) times during a shutdown.
6. Reoxidation of sulfide can be important to the net reduction efficiency obtained. As the smelt flows toward the spouts and out of the furnace it has an opportunity to come in contact with the large quantities of primary air introduced at a level just above the smelt. This can reoxidize some of the sulfide, and will also increase smelt temperature. A large char bed can act as a shield and help minimize reoxidation.
7. The same reaction that is responsible for sulfate reduction is responsible for gasification and combustion of char. The sulfate is the main oxygen carrier to the char, and a sulfate-sulfide oxidation-reduction cycle can effectively lead to the exothermic combustion of the char by air. This implies that the activation energy for char combustion is about 50 kcal/mole  $\text{Na}_2\text{SO}_4$  (12.5 to 25 kcal/mole C, depending on stoichiometry). It also implies that char combustion has a threshold temperature of about 1500°F, below which reaction is very slow.

#### FUTURE WORK

The future work planned in the study of sulfate reduction with carbon can be divided into two areas: laboratory studies with kraft char and field studies. The reduction experiments with carbon rods enabled the basic mechanism of sulfate reduction to be determined. Future laboratory studies with char as the source of carbon will enable the model presented in this report to be expanded to a system which more closely simulates the environment of a kraft recovery furnace.

The second area of future research involves actual measurements on kraft recovery furnaces. Those measurements will include temperature, degree of reduction, and carbon dioxide/carbon monoxide profiles in the bed of a kraft recovery furnace. These measurements will aid in determining the applicability of the mechanism presented in this report to the processes occurring in a kraft recovery furnace.

#### ACKNOWLEDGMENTS

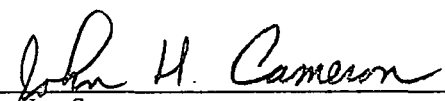
The authors wish to acknowledge the contributions of Bruce D. Andrews, who obtained a considerable amount of the data contained in this report, Orlin G. Kuehl for design and construction of the experimental apparatus, and Donald G. Sachs for his excellent analysis of melt samples.


LITERATURE CITED

1. White, J. F. M. and White, A. H. Reduction of sodium sulfate to sodium sulfide at temperatures below 800°C. Ind. Eng. Chem. 28(2):244-6(Feb. 1936).
2. Polyvyanni, T. R. and Demchenko, R. S. The rate of reduction of sodium sulfate. Izvest. Akad. Nauk Kazakh. SSR Ser. Met. Obogaschchen i Ognenporov (2):34-42(1960).
3. Panushev, T. and Ivanov, D. G. Intense reduction of sodium sulfate of solid and liquid reducing agents. God. Vissh. Khimikotechnol. Inst. Sofia 15(4):133-45(1970).
4. Birk, J. R., Larsen, C. M., Vaux, W. G., and Oldenkamp, R. D. Hydrogen reduction of alkali sulfate. Ind. Eng. Chem., Process Design Devt. 10(1):7-13 (1971).
5. Nikitin, V. A. and Kunian, T. I. Mechanism of the reduction of sodium sulfate with carbon. Zh. Vses. Khim. Obshchest. D.I. Mendeleeva 5:350-2(1960).
6. Budnikoff, P. P. and Shilov, E. The reduction of sodium sulfate to sulfide. J. Soc. Chem. Ind. 111-13T(April 1928).
7. Nyman, C. J. and O'Brien, T. D. Catalytic reduction of sodium sulfate. Ind. Eng. Chem. 8:1019-21(August 1947).
8. Kunin, V. T. and Kirillov, I. P. Izv. Vyssh. Ucheb. Zaved., Khim. Khim. Tekhnol. 11(5):569-72(1968).
9. Borg, A., Teder, A., and Warnqvist, B. Inside a kraft recovery furnace - studies on the origins of sulfur and sodium emissions. Tappi 57(1):126-9(Jan. 1974).
10. Richardson, D. L. and Merriam, R. L. Study of cooling and smelt solidification in black liquor recovery boilers. Phase I, Report for American Paper Institute, Arthur D. Little Inc., Cambridge, Mass. (Feb. 1977).
11. Richardson, D. L. and Merriam, R. L. A study of black liquor recovery furnace firing conditions, char bed characteristics and performance. Phase II, Report for American Paper Institute, Arthur D. Little Inc., Cambridge, Mass. (Dec. 1978).
12. Stelman, D., Darnell, A. J., Christie, J. R., and Yosim, S. J. Air Oxidation of Graphite in Molten Salts. In Molten Salts, Pemsler, J. P., et al. ed., published by The Electrochemical Society, Princeton, NJ, 1976. p. 299-314.




THE INSTITUTE OF PAPER CHEMISTRY

  
\_\_\_\_\_  
John H. Cameron  
Research Associate  
Chemical Recovery  
Chemical Sciences Division

  
\_\_\_\_\_  
Thomas M. Grace  
Group Leader, Recovery  
Pulping Sciences  
Chemical Sciences Division

Approved by

  
\_\_\_\_\_  
Earl W. Malcolm  
Director  
Chemical Sciences Division

IPST HASELTON LIBRARY



5 0602 01056343 7